B E R I C H T E

AUS DEM

INSTITUT FÜR MEERESKUNDE

AN DER

CHRISTIAN-ALBRECHTS-UNIVERSITÄT KIEL

NR. 104

DOI 10.3289/IFM_BER_104

A DETAILED DESCRIPTION OF A SEMISPECTRAL MODEL ON THE β-PLANE

VON

W. KRAUSS & CH. WÜBBER

1982

PART 1:

ANALYTICAL FORMALISM

Summary: A semispectral model on the β-plane.
Part 1: Analytical treatment

Part 1 of this paper deals with the development of a linear β-plane model for a rectangular basin of constant depth. Spectral methods are applied whenever they turn out to be more efficient and more accurate than grid point methods. The solution is obtained by adding a free solution to the forced one in order to fulfill the horizontal boundary conditions. The forces applied are windstress and air-pressure. The forced solution uses Fourier decomposition with respect to x, y and t and numerical integration with respect to z. This solution is vertically decomposed into the eigenfunctions at the horizontal boundaries. The free solution is obtained by Fourier decomposition of each mode with respect to y and t and numerical integration with respect to x. Part 2 deals with the numerical methods and demonstrates the efficiency of the model.

Zusammenfassung: Ein Semispektralmodell auf der β-Ebene.
Teil 1: Analytischer Teil

Im 1. Teil dieser Abhandlung werden die analytischen Grundlagen für ein Ozeanmodell auf der β-Ebene bereitgestellt. Der Ozean sei ein rechteckiges Becken konstanter Tiefe. Spektralmethoden werden immer dann angewandt, wenn sie effizienter und genauer sind als Gitterpunktmethoden. Zur Erfüllung der horizontalen Randbedingungen wird zur erzwungenen Lösung eine freie hinzu addiert. Die erzwungene Lösung resultiert

aus der tangentialen Schubspannung des Windes und dem Luftdruck. Sie wird durch Fourierzerlegung bezüglich x, y und t sowie numerischer Integration bezüglich z erhalten. An den horizontalen Rändern wird diese Lösung nach Eigenfunktionen der Dichteschichtung zerlegt. Die freie Lösung wird spektral bezüglich y, t und z und durch numerische Integration bezüglich x erhalten. Im 2. Teil dieser Arbeit werden die numerischen Methoden behandelt, und es wird an Hand von Beispielen die Effizienz des Modelles demonstriert.

1. Introduction

Efficient and accurate numerical methods for modeling the large-scale ocean circulation are important for understanding ocean dynamics. Several approaches have been used. Most models presently used fall into the class of grid point models (e.g. Bryan (1963, 1969), Simons (1973), Hansen (1956)) where the differential quotients with respect to any independent variable are approximated by difference methods.

These models have proven to be very powerful in some respect. Their disadvantages with respect to ocean models are:

i) they are very time consuming; especially if a steady state should be described

ii) they have a tendency towards phase errors due to the horizontal gridding

iii) they require, in general, a large horizontal eddy viscosity or a numerical smoothing procedure in order to give stable solutions. As a consequence, these models are rather diffusive.

Spectral models first developed in meteorology, are much less sensitive to the restrictions ii) and iii). Due to the spectral decomposition in space layered models require only a time integration of the spectral coefficient which makes them fast. Deficiencies of spectral models are mainly due to the non-linear terms. Most of them have been overcome during recent years. A very detailed account of the work done in meteorology is due to Machenhauer (1979).

In oceanography spectral models have not been used very often. The models of Heaps (1972) and Davis (1979) use spectral decomposition with respect to the frictional operator in the vertical coordinate and grid points with respect to the remaining coordinates.

The approach in eddy resolving models (Haidvogel et al., 1980), which have been restricted to rectangular areas of constant depth, is similar to that in meteorology (Machenhauer, 1979). The main difference is that often Chebyshew polynomials are used in oceanography in order to handle the horizontal boundary problem.

A different approach has been used by one of the authors (Krauss, 1976) on a f-plane where all variations with respect to the horizontal coordinates and time are Fourier decomposed and the grid point method is retained with regard to the vertical coordinate only. This method is especially appropriate with respect to wave-like features because the dispersion relations are exactly retained. The incorporation of bottom topography could be handled by adding free solutions of the system of equations (Krauss, 1979).

The present model is an extension of that described above, applied to the β-plane. In the present version, it is linear and applied to a rectangular basin of constant depth. The incorporation of arbitrary bottom topography and an arbitrary shape of the coast line could be achieved by similar methods as mentioned above. This, however, is beyond the scope of the present paper.

The model is semispectral because it uses spectral expansions with respect to those coordinates for which an expansion is most appropriate. We decompose the solution into two parts:

i) a forced solution which is obtained by Fourier expansion with respect to x, y and t. The integration with respect to z is done numerically in order to allow an easy incorporation of arbitrary eddy viscosities and density stratification.

ii) a free solution which is added in order to fulfill the horizontal boundary conditions. This free solution yields the westward intensification. If we would use a Fourier-decomposition with respect to the east-west-coordinate for this solution we would have to use a large number of Fourier components. To avoid this, the spectral method is used only with respect to y, t and z, where the variations in z are decomposed into the eigenfunctions of the stratified fluid. Grid point methods are used to perform the x-integration.

The model, at least in its linear version, is extremely fast. This is achieved by Fourier expanding also the time domain. Most problems in large-scale oceanography are concerned with a quasi-steady state or with low frequency motions. Contrary to time step methods, for which integrations over long time ranges have to be performed in order to reach a quasisteady state, the solution in the present model is obtained by superposition of a few frequency bands. A Stommel-type solution for a constant windstress in x-direction which varies according

to cos ηy , requires only about 60 sec computer time on a CYBER 76. In this case, the ocean is stratified and the vertical variations are resolved by 200 grid points.

2. The β-plane model

We consider a rectangular basin of dimensions X (east-west width) and Y (north-south width). The coordinate system is right-handed with x towards west, y towards north and z downwards. The depth is assumed to be constant (H) (fig. 1). The Coriolis parameter, $f = f_o + \beta y$ is a linear function of the north-south coordinate, f_o and β have mid-latitude values.

As a basic state, we prescribe the mean density $\bar{\rho}(z)$.

The ocean is driven by windstress and air-pressure variations at the sea surface; frictional dissipation occurs in the interior and at the bottom. The eddy viscosity μ(z) which transfers momentum from the surface into the interior, is prescribed. Horizontal eddy viscosity is neglected. At the horizontal boundaries x = 0 and x = X, which are assumed to be rigid walls, we allow free slip. The boundaries at y = 0 and y = Y are assumed to be open boundaries.

2.1. The basic state and the governing equations

The basic state is an ocean at rest with continuous stratification $\bar{\rho}(z)$. Pressure $\bar{p}(z)$ is given by the static equation

$$(2.1.1) \qquad \frac{d\bar{p}}{dz} = g\bar{\rho}$$

2.2. The perturbation equations

Deviations from the basic state due to the forces applied are considered to be linear motions. Thus, we have

$$(2.2.1) \quad \frac{\partial u}{\partial t} + (f_o+\beta y)\, v - \frac{\partial}{\partial z}\left(\mu \frac{\partial u}{\partial z}\right) + \frac{\partial P}{\partial x} = 0$$

$$(2.2.2) \quad \frac{\partial v}{\partial t} - (f_o+\beta y)\, u - \frac{\partial}{\partial z}\left(\mu \frac{\partial v}{\partial z}\right) + \frac{\partial P}{\partial y} = 0$$

$$(2.2.3) \quad - gR + \frac{\partial P}{\partial z} + \Gamma P = 0$$

$$(2.2.4) \quad \frac{\partial R}{\partial t} + \Gamma w = 0$$

$$(2.2.5) \quad \frac{\partial u}{\partial x} + \frac{\partial v}{\partial y} + \frac{\partial w}{\partial z} = 0$$

where

$$(2.2.6) \qquad P = \frac{p}{\bar{\rho}} \qquad R = \frac{\rho}{\bar{\rho}}$$

and

$$(2.2.7) \qquad \Gamma(z) = \frac{1}{\bar{\rho}} \frac{d\bar{\rho}}{dz}$$

is the stability parameter ($g\Gamma = N^2$ is the Brunt-Väisälä frequency).

Combining (2.2.3) - (2.2.5) we arrive at

$$(2.2.8)\qquad \frac{\partial}{\partial t}\left[\frac{\partial^2 P}{\partial z^2} + \left(\Gamma - \frac{\Gamma'}{\Gamma}\right)\frac{\partial P}{\partial z}\right] - g\Gamma\left(\frac{\partial u}{\partial x} + \frac{\partial v}{\partial y}\right) = 0$$

where $\Gamma' = \partial\Gamma/\partial z$.

Instead of using (2.2.1), (2.2.2) we introduce divergence D and vorticity ξ

$$(2.2.9)\qquad D = \frac{\partial u}{\partial x} + \frac{\partial v}{\partial y} \qquad\qquad \xi = \frac{\partial v}{\partial x} - \frac{\partial u}{\partial y}.$$

Thus, (2.2.1) and (2.2.2) are replaced by

$$(2.2.10)\qquad \frac{\partial D}{\partial t} + f_o\xi - \beta u - \frac{\partial}{\partial z}\left(\mu\frac{\partial D}{\partial z}\right) + \Delta P = 0$$

$$(2.2.11)\qquad \frac{\partial \xi}{\partial t} - f_o D - \beta v - \frac{\partial}{\partial z}\left(\mu\frac{\partial \xi}{\partial z}\right) = 0$$

where Δ is the horizontal Laplacean ($\Delta = \frac{\partial^2}{\partial x^2} + \frac{\partial^2}{\partial y^2}$).

Finally, introducing a stream function ψ and a velocity potential ϕ

$$(2.2.12)\qquad u = -\frac{\partial \phi}{\partial x} + \frac{\partial \psi}{\partial y}\,, \qquad v = -\frac{\partial \phi}{\partial y} - \frac{\partial \psi}{\partial x}$$

$$(2.2.13)\qquad D = -\Delta\phi\,, \qquad \xi = -\Delta\psi$$

we arrive at

$$(2.2.14)\qquad -\frac{\partial}{\partial t}\Delta\phi - f_o\Delta\psi + \beta\frac{\partial \phi}{\partial x} - \beta\frac{\partial \psi}{\partial y} + \frac{\partial}{\partial z}\left(\mu\frac{\partial}{\partial z}\Delta\phi\right) + \Delta P = 0$$

$$(2.2.15)\quad -\frac{\partial}{\partial t}\Delta\psi + f_o\Delta\phi + \beta\frac{\partial\phi}{\partial y} + \beta\frac{\partial\psi}{\partial x} + \frac{\partial}{\partial z}\left(\mu\frac{\partial}{\partial z}\Delta\psi\right) = 0$$

$$(2.2.16)\quad \frac{\partial}{\partial t}\left\{\frac{\partial^2 P}{\partial z^2} + \left(\Gamma - \frac{\Gamma'}{\Gamma}\right)\frac{\partial P}{\partial z}\right\} + g\Gamma\Delta\phi = 0$$

Equs. (2.2.14) - (2.2.15) are tendency equations for divergence, vorticity and pressure.

2.3. The boundary conditions

The boundary conditions at the sea surface z = 0 are

$$(2.3.1)\quad \mu\frac{\partial u}{\partial z} = -\tau^{(x)},\ \mu\frac{\partial v}{\partial z} = -\tau^{(y)},\ P = P_o + g\zeta\ ,\ w = -\frac{\partial\zeta}{\partial t}\quad \text{for } z = 0$$

where $\vec{\tau} = (\tau^{(x)},\tau^{(y)})$ is windstress, P_o air-pressure divided by surface density and ζ the free surface. At the bottom we assume the stress to be proportional to the bottom velocities,

$$(2.3.2)\quad \frac{\partial u}{\partial z} = -ru\ ,\quad \frac{\partial v}{\partial z} = -rv,\quad w = 0\quad \text{for } z = H,$$

where r is a friction coefficient ($r > 0$).

By applying divergence and curl to the first two equations (2.3.1) we obtain the corresponding relations for ϕ and ψ. The last two equations of (2.3.1) give a relation between P and w; the latter can be eliminated by means of (2.2.3) and (2.2.4), which yields

$$(2.3.3)\quad w = -\frac{1}{g\Gamma}\frac{\partial}{\partial t}\left(\frac{\partial P}{\partial z} + \Gamma P\right).$$

We thus obtain

$$(2.3.4)\quad \frac{\partial}{\partial z}\Delta\phi = \frac{1}{\mu}\left(\frac{\partial\tau^{(x)}}{\partial x} + \frac{\partial\tau^{(y)}}{\partial y}\right),\ \frac{\partial}{\partial z}\Delta\psi = \frac{1}{\mu}\left(\frac{\partial\tau^{(y)}}{\partial x} - \frac{\partial\tau^{(x)}}{\partial y}\right)\quad \text{for } z = 0$$

$$(2.3.5) \qquad \frac{\partial P}{\partial z} = -\frac{\Gamma}{\bar{\rho}} P_o \quad \text{for } z = 0$$

and, similarly,

$$(2.3.6) \qquad \frac{\partial}{\partial z}\Delta\phi = -r\Delta\phi \quad , \quad \frac{\partial}{\partial z}\Delta\psi = -r\Delta\psi \quad , \quad \frac{\partial P}{\partial z} + \Gamma P = 0 \quad \text{for } z = H.$$

At the rigid walls $x = 0$ and $x = X$ we have $u = 0$, which, by means of (2.2.12), yields

$$(2.3.7) \qquad -\frac{\partial \phi}{\partial x} + \frac{\partial \psi}{\partial y} = 0 \quad \text{at } x = 0 \text{ and } x = X.$$

As mentioned before, the boundaries at $y = 0$ and $y = Y$ are treated as open boundaries where the flow may enter or leave the area according to the prescribed wind field, which is periodic with respect to y (and thus the solutions are). The forces are considered to be even functions of y.

2.4. Equations in the Fourier Space

As outlined in section 3.2, the solution to the system (2.2.14) - (2.2.16) with (2.3.4) - (2.3.7) will be obtained by superposition of a forced solution due to the driving forces and a free solution in order to fulfill the boundary conditions. The forced solution is obtained in the Fourier space with respect to x, y and t. For that purpose we have to transform the system into the Fourier domain. The z-dependency is retained in order to solve the system for any prescribed vertical distribution of eddy viscosities.

Each of the fields ϕ, ψ, and P is expanded into a finite Fourier series

$$(2.4.1)\quad \chi(x,y,z,t) = \sum_{m=-M}^{M} \sum_{k=-K}^{k} \sum_{\ell=-L}^{L} \tilde{\chi}(\kappa_k,\eta_\ell,\omega_m,z)\, e^{i(\kappa_k x+\eta_\ell y+\omega_m t)}$$

where

$$(2.4.2)\quad \tilde{\chi} = \chi_1 + i\chi_2, \quad \kappa_k = k\kappa_o, \text{ etc.}$$

The corresponding Fourier coefficients of the driving forces are denoted by

$$(2.4.3)\quad \tilde{\tau}^{(x)} = T_1 + iT_2 \qquad \tilde{\tau}^{(y)} = T_3 + iT_4 \qquad \tilde{P}_o = T_5 + iT_6$$

Applying (2.4.1) to the system (2.2.14) - (2.2.16) we obtain a coupled system of second order differential equations in z (indices k, ℓ, m are omitted and $k^2 = \kappa^2 + \eta^2$):

$$(2.4.4)\quad \frac{\partial^2\tilde{\phi}}{\partial z^2} + \frac{\mu'}{\mu}\frac{\partial\tilde{\phi}}{\partial z} - i\,\frac{\omega+\beta\frac{\kappa}{k^2}}{\mu}\,\tilde{\phi} - \left(\frac{f_o}{\mu} - \frac{i\beta\eta}{k^2\mu}\right)\tilde{\psi} + \frac{1}{\mu}\tilde{P} = 0$$

$$(2.4.5)\quad \frac{\partial^2\tilde{\psi}}{\partial z^2} + \frac{\mu'}{\mu}\frac{\partial\tilde{\psi}}{\partial z} - i\,\frac{\omega+\beta\frac{\kappa}{k^2}}{\mu}\,\tilde{\psi} + \left(\frac{f_o}{\mu} - \frac{i\beta\eta}{k^2\mu}\right)\tilde{\phi} = 0$$

$$(2.4.6)\quad \frac{\partial^2\tilde{P}}{\partial z^2} + \left(\Gamma - \frac{\Gamma'}{\Gamma}\right)\frac{\partial\tilde{P}}{\partial z} + i\,\frac{g\Gamma k^2}{\omega}\,\tilde{\phi} = 0$$

with

$$(2.4.7)\quad \frac{\partial\tilde{\phi}}{\partial z} = -\frac{i}{\mu k^2}\,(\kappa\tilde{\tau}(x)+\eta\tilde{\tau}(y)) \qquad \frac{\partial\tilde{\psi}}{\partial z} = -\frac{i}{\mu k^2}\,(\kappa\tilde{\tau}(y)-\eta\tilde{\tau}(x)) \qquad \text{for } z = 0$$

$$(2.4.8)\quad \frac{\partial\tilde{P}}{\partial z} = -\frac{\Gamma}{\bar{\rho}}\,\tilde{P}_o \qquad \text{for } z = 0$$

$$(2.4.9)\quad \frac{\partial\tilde{\phi}}{\partial z} = -r\tilde{\phi} \qquad \frac{\partial\tilde{\psi}}{\partial z} = -r\tilde{\psi} \qquad \frac{\partial\tilde{P}}{\partial z} + \Gamma\tilde{P} = 0 \qquad \text{at } z = H$$

The system has to be solved for the entire domain $-K<\kappa<K$, $-L<\eta<+L$, $-M<\omega<M$; the complete solution is obtained by superposition according to (2.4.1). Terms due to $\kappa = 0$, $\eta = 0$, and $\omega = 0$ are excluded.

Higher accuracy with respect to the numerics is obtained by solving (2.4.4) - (2.4.6) for the real coefficients χ_1 and χ_2. In this case, we get six equations instead of three and the final solution corresponding to (2.4.1) may conveniently be written in the form

$$(2.4.10)\quad \chi(x,y,z,t) = 2\sum_{m=1}^{M}\Big\{\sum_{k=-K}^{K}\sum_{\ell=-L}^{L}\big[\chi_1(\kappa_k,\eta_\ell,\omega_m,z)\cos(\kappa_k x+\eta_\ell y)$$

$$-\chi_2(\kappa_k,\eta_\ell,\omega_m z)\sin(\kappa_k x+\eta_\ell y)\big]\cos\omega_m t$$

$$-\big[\chi_2(\kappa_k,\eta_\ell,\omega_m,z)\cos(\kappa_k x+\eta_\ell y)+\chi_1(\kappa_k,\eta_\ell,\omega_m,z)\sin(\kappa_k x+\eta_\ell y)\big]\sin\omega_m t\Big\}$$

where the summation with respect to m extends over the positive range only. This results from the reality condition of the functions χ.

The equations corresponding to (2.4.4) - (2.4.9) are

$$
(2.4.11)\quad \begin{cases}
\dfrac{d^2\phi_{1,2}}{dz^2} + \dfrac{\mu'}{\mu}\dfrac{d\phi_{1,2}}{dz} \pm \left(\dfrac{\omega}{\mu} + \dfrac{\beta\kappa}{\mu k^2}\right)\phi_{2,1} - \dfrac{f_o}{\mu}\psi_{1,2} \mp \dfrac{\beta\eta}{k^2\mu}\psi_{2,1} + \dfrac{1}{\mu}P_{1,2} = 0 \\[2ex]
\dfrac{d^2\psi_{1,2}}{dz^2} + \dfrac{\mu'}{\mu}\dfrac{d\psi_{1,2}}{dz} \pm \left(\dfrac{\omega}{\mu} + \dfrac{\beta\kappa}{\mu k^2}\right)\psi_{2,1} + \dfrac{f_o}{\mu}\phi_{1,2} \pm \dfrac{\beta\eta}{k^2\mu}\phi_{2,1} = 0 \\[2ex]
\dfrac{d^2P_{1,2}}{dz^2} + \left(\Gamma - \dfrac{\Gamma'}{\Gamma}\right)\dfrac{dP_{1,2}}{dz} \mp \dfrac{g\Gamma k^2}{\omega}\phi_{2,1} = 0
\end{cases}
$$

with

$$
(2.4.12)\quad \begin{cases}
\dfrac{d\phi_{1,2}}{dz} = \pm\dfrac{1}{\mu k^2}\left(\kappa T_{2,1} + \eta T_{4,3}\right) \\[2ex]
\dfrac{d\psi_{1,2}}{dz} = \mp\dfrac{1}{\mu k^2}\left(\eta T_{2,1} - \kappa T_{4,3}\right) \qquad \text{at } z = 0 \\[2ex]
\dfrac{dP_{1,2}}{dz} = -\dfrac{\Gamma}{\bar{\rho}} T_{5,6}
\end{cases}
$$

and

$$(2.4.13)\qquad \frac{d\phi_{1,2}}{dz} = -r\phi_{1,2} \qquad \frac{d\psi_{1,2}}{dz} = -r\psi_{1,2} \qquad \text{at } z = H$$

$$\frac{dP_{1,2}}{dz} + \Gamma P_{1,2} = 0$$

3. System behaviour

Before handling the full set of equations, we first consider a simplified version in order to discuss the major physics involved and in order to outline the procedure by which the system is solved.

3.1. The simplified system for low frequencies

For low frequencies, $\omega \ll f_o$, the system responds quasi-geostrophic. In (2.2.14) the main balance is between term 2 and 6, in (2.2.15) between 1, 2, 4 and 5 depending on whether we consider barotropic or baroclinic motions, and in (2.2.16) between 1 and 4. Thus, we have the simplified system (μ = const, Γ = const)

$$(3.1.1)\qquad f_o\psi = P$$

$$(3.1.2)\qquad -\frac{\partial}{\partial t}\Delta\psi + f_o\Delta\phi + \beta\frac{\partial\psi}{\partial x} + \mu\frac{\partial^2}{\partial z^2}\Delta\psi = 0$$

$$(3.1.4)\qquad \frac{\partial}{\partial t}\frac{\partial^2 P}{\partial z^2} + g\Gamma\Delta\phi = 0$$

which yields one equation for the stream function,

$$(3.1.5)\quad -\frac{\partial}{\partial t}\left(\Delta\psi + \frac{f_o^2}{g\Gamma}\frac{\partial^2\psi}{\partial z^2}\right) + \beta\frac{\partial\psi}{\partial x} + \mu\frac{\partial^2}{\partial z^2}\Delta\psi = 0$$

As outlined in detail in section 3.2., the forced solution is obtained in the Fourier space. The periodic solutions of (3.1.5) are, therefore, essential. In the inviscid case, $\mu = 0$, this equation describes Rossby waves. The barotropic ones, $\partial/\partial z = 0$, are given by

$$(3.1.6)\qquad -\frac{\partial}{\partial t}\Delta\psi + \beta\frac{\partial\psi}{\partial x} = 0.$$

Assuming $\psi \sim e^{i(\kappa x+\eta y-\omega t)}$, i.g. the waves travelling towards west, the dispersion relation is

$$(3.1.7)\qquad \omega = \frac{\beta\kappa}{k^2}, \qquad k^2 = \kappa^2 + \eta^2.$$

Baroclinic waves in an exponentially stratified fluid are given by $\psi \sim \cos(\frac{n\pi}{H} z)\, e^{i(\kappa x+\eta y-\omega t)}$, and we obtain from the terms 1 - 3

$$(3.1.8)\qquad \omega = \frac{\beta\kappa}{k^2 + \frac{f_o^2}{g\Gamma}\left(\frac{n\pi}{H}\right)^2},$$

the well-known dispersion relationship.

If viscosity is taken into account, the vertical structure of periodic solutions is governed by

$$(3.1.9)\quad \left(\mu k^2 - \frac{i\omega f_o^2}{g\Gamma}\right)\frac{\partial^2\psi}{\partial z^2} - i(\beta\kappa - \omega k^2)\psi = 0$$

For large-scale forcing ($\kappa \approx 10^{-8}$) at low frequencies, $\omega k^2 << \beta\kappa$, and may be neglected. The response depends essentially on the ratio between μk^2 and $\omega f_o^2/g\Gamma$. If $\mu k^2 << \frac{\omega f_o^2}{g\Gamma}$, i.e. $\omega >> \mu k^2\, g\Gamma/f_o^2$, the solution is approximately

$$(3.1.10)\qquad \psi \sim e^{\pm i\sqrt{\frac{\beta\kappa g\Gamma}{\omega f_o^2}}\, z}$$

Choosing $g\Gamma = 10^{-5}$, $\beta = 10^{-13}$, $f_o^2 = 10^{-8}$, $\kappa = n\kappa_o = 0.5n\ 10^{-8}$ we arrive at $\omega >> \mu n^2\ 10^{-13}$. Thus, (3.1.1o) is a good approximation for low wave numbers ($n<10$) and eddy viscosities $1<\mu< 10^2$, if we are concerned with frequencies $\omega > 10^{-9}$ ($\tau<200$ years).

The exponent in (3.1.10) is essentially constant for $\omega>10^{-7}$ and $z < 4\cdot10^5$. Thus, the response is barotropic for periods $\tau \leq 1$ year and becomes increasingly baroclinic for longer periods. The same has been shown by G. Veronis & H. Stommel (1956) for a two-layered ocean and by J. Willebrand et al. (1978) for a continuously stratified one.

The solution becomes different if the motion becomes quasi-steady ($\omega\to0$). Equ. (3.1.9) then reduces to

$$(3.1.11)\qquad \frac{\partial^2\psi}{\partial z^2} - \frac{i\beta\kappa}{\mu k^2}\psi = 0$$

the solution of which is

$$(3.1.12) \qquad \psi \sim e^{\pm (1+i)\sqrt{\frac{\beta\kappa}{2\mu k^2}}\, z}$$

In this case, the motion is concentrated near the surface. The energy which is supplied by the wind, accelerates the surface layer and inclines the density surfaces below that layer which compensates the entire pressure field of the surface layer. The lower layers remain at rest; all of the work done by upper layer pressure forces is converted into available potential energy. In the non-linear case, the vertical shears associated with this process, yield baroclinic instability which allows meso-scale eddies to develop and transfer energy into kinetic energy of the deeper layers (Holland & Lin, 1975). In the linear case, the deep layers stay at rest. The problem has been discussed by Charney & Flierl (1981) and Young (1981).

The limitations of the model in the frequency range are, therefore, mainly due to (2.2.4). For extremely low frequencies, horizontal advection and vertical mixing of density can no longer be neglected. We exclude this case in the present paper. Then, the simplified set of equs. (3.1.1) - (3.1.4) describe mainly three processes

i) barotropic Rossby waves
ii) baroclinic Rossby waves
iii) the large-scale barotropic and baroclinic flow field due to external forcing for periods up to several decades.

The complete set,(2.4.11), additionally contains the modifications due to minor terms.

3.2. Mathematical procedure of solving the equations

Compared to the f-plane,spectral models on a β-plane exhibit the disadvantage that due to the β-term the solutions

are phase-shifted with respect to x compared to the wind field. They, therefore, do not fulfill the horizontal boundary conditions even if the wind stress does.

To overcome the problem, we proceed as follows:

i) we first compute a solution due to the prescribed external forces which fulfills the boundary conditions at the surface (z = 0) and the bottom (z = H). This solution is called the forced solution; it does not fulfill the horizontal boundary conditions at x = 0 and x = X.

ii) we then expand the solution ψ at x = 0 and x = X into eigenfunctions with respect to z and Fourier series with respect to y and t, and determine the amplitudes of these eigenfunctions.

iii) the equations (2.2.14) - (2.2.16) are expanded into the same system of eigenfunctions, which has the properties

$$\frac{\partial u}{\partial z} = \frac{\partial v}{\partial z} = \frac{\partial P}{\partial z} = 0 \quad \text{at } z = 0$$

and, thus, does not alter the boundary conditions already applied. This yields a set of second-order differential equations for the amplitudes of the eigenfunctions with respect to x (spectral equations) which is solved numerically. The boundary conditions at x = 0 and x = X are chosen such that the sum of these solutions and the free solutions expanded under ii) fulfill the real boundary conditions.

These solutions are called free solutions (due to the fact that these are solutions of the homogeneous set of equations not being directly influenced by external forces. We could solve the system for arbitrary horizontal boundary values and afterwards determine the amplitude in such a way as to fulfill the real boundary condition).

The procedure may be outlined by solving the steady Stommel-problem (STOMMEL, 1948) for the vertically integrated equations. The problem then is to solve the vertically averaged equation (3.1.5)

$$(3.2.1) \qquad K_H \Delta\bar{\psi} - \beta \frac{\partial\bar{\psi}}{\partial x} = \frac{1}{\bar{H}} \frac{\partial \tau^{(x)}}{\partial y} \qquad \text{with } \psi = 0 \text{ at } x = 0,\ x = X$$

where $K_H = r\mu/H$ and in the second equation of (2.3.6) ψ has been replaced by its averaged value $\bar{\psi}$. The wind field is the classical one, here represented by one Fourier component with respect to x,

$$(3.2.2) \qquad \frac{\tau^{(x)}}{\bar{H}} = \tau_o \sin \kappa x \cos \eta y.$$

The solution is obtained by assuming

$$(3.2.3) \qquad \bar{\psi} = [\psi_1(x) + \psi_2(x)] \sin \eta y,$$

where ψ_1 is the forced and ψ_2 the free solution. This yields for the forced problem

$$(3.2.4) \qquad \frac{\partial^2\psi_1}{\partial x^2} - \frac{\beta}{K_H} \frac{\partial\psi_1}{\partial x} - \eta^2\psi_1 = - \frac{\eta\tau_o}{K_H} \sin \kappa x$$

the solution of which is

$$(3.2.5) \qquad \psi_1 = \frac{\tau_o \eta}{K_H\left(k^4 + \frac{\beta^2\kappa^2}{K_H^2}\right)} \left\{ k^2 \sin \kappa x - \frac{\beta\kappa}{K_H} \cos \kappa x \right\} \quad , k^2 = \kappa^2+\eta^2 .$$

It does not fulfill the boundary condition (3.2.1) due to the β-term which shifts the solution towards the west (fig. 2).

The <u>free solution</u> takes care of the boundary conditions:

$$(3.2.6) \qquad \frac{\partial^2\psi_2}{\partial x^2} - \frac{\beta}{K_H}\frac{\partial\psi_2}{\partial x} - \eta^2\psi_2 = 0 \qquad \text{with} \quad \psi_2(0) = -\psi_1(0)$$
$$\psi_2(X) = -\psi_1(X)$$

The solution to (3.2.6) is of the type

$$(3.2.7) \qquad \psi_2 = a \sin \kappa x + b \cos \kappa x$$

where

$$(3.2.8) \qquad \kappa^4 + \left(2\eta^2 + \frac{\beta^2}{K_H^2}\right) \kappa^2 + \eta^4 = 0.$$

Approximate solutions to this are

$$(3.2.9) \qquad \kappa_{1,2} \approx \pm \frac{i\beta}{K_H} \; (\approx 10^{-7}) \qquad\qquad \kappa_{3,4} \approx \pm \frac{i\eta^2 K_H}{\beta} \; (\approx 10^{-9})$$

The roots $\kappa_{1,2}$ describe the westward intensification, $\kappa_{3,4}$ the Sverdrup regime.

Substitution of (3.2.9) into (3.2.7) and determining the amplitudes a_i, b_i $(i=1,\ldots,4)$, we obtain for $\eta^2 K_H^2 \ll \beta^2$

$$\psi_2 = -\psi_1(o)\,\frac{(1 + e^{\frac{\beta X}{K_H}})\, e^{-\frac{\eta^2 K_H X}{\beta}\frac{x}{X}} - (1 + e^{-\frac{\eta^2 K_H X}{\beta}})\, e^{\frac{\beta X}{K_H}\frac{x}{X}}}{e^{\frac{\beta X}{K_H}} - e^{-\frac{\eta^2 K X}{\beta}}}$$

This is also displayed in Fig. 2. The sum of both yields the total solution (fig. 2) for one component of the wind field. The Stommel solution is obtained by superposition of all Fourier components. (Fig. 2 is based on $\kappa_o = 0.5\ 10^{-8} cm^{-1}$, $\eta_o = 10^{-8}\ cm^{-1}$, $K_H = 10^{-6}\ s^{-1}$. For $H = 10^5$ cm ψ is in $10^8\ cm^2 s^{-1}$ units)

3.3. The dispersion relation

As mentioned in section 3.1., the model is well suited to describe the entire set of Rossby waves. This is especially so because the model requires no horizontal eddy viscosity for stability reasons. Thus, Rossby waves will always be generated (like inertial waves on the f-plane) if Fourier-components of the wind field contain energy near the dispersion lines of the Rossby waves. The response then is dependent on the internal friction of the system, but maximum response occurs in the vicinity of the dispersion lines which are plotted in Fig. 4 for the density distribution displayed in Fig. 3. The density resembles the mean stratification of the North Atlantic Ocean in the Azores area, which is chosen as being representative for the basic state of the North Atlantic Ocean.

In Fig. 4 we additionally characterize the wavenumber range with respect to x which contains the main energy of the wind field for an ocean of a width of about 6000 km. β has been given a mean latitude value of $1.6 \cdot 10^{-13}$ which corresponds to a latitude of ϕ = 45 N. Under these conditions the ocean responds barotropically to annual forcing and baroclinically for longer periods. If the β-plane is attached at lower latitudes in order to describe processes there, β would increase and f decrease. According to (3.1.8), the dispersion lines of the baroclinic modes would be shifted towards higher frequencies and the first baroclinic mode is exaggerated already by annual variations of the external forces (Krauss & Wübber, 1982).

4. Expansion of the free wave equations and of the boundary conditions into eigenfunctions

As outlined in section 3.2, the free solutions will be obtained by mode decomposition with respect to z and horizontal interpretation with respect to x. Variations in y and t are Fourier decomposed.

4.1. The eigenfunctions

In a stratified inviscid fluid, the horizontal components of the velocity field can be expanded into eigenfunctions of the pressure field (W. Krauss, 1966; P. LeBlond & L. Mysak, 1977). Problems arise from a proper treatment of the friction terms in case of a viscous fluid. We come back to that problem in section 4.3.

The eigenfunction problem results from equ. (2.2.8) which may be written in the form

$$(4.1.1) \qquad \frac{\partial}{\partial z}\left[\frac{1}{g\Gamma}\frac{\partial}{\partial t}\left(\frac{\partial P}{\partial z}+\Gamma P\right)\right]-\left(\frac{\partial u}{\partial x}+\frac{\partial v}{\partial y}\right)=0$$

Assuming

$$(4.1.2) \qquad P=\tilde{P}(x,y,t)Z(z), \qquad u=\tilde{u}(x,y,t)Z(z), \qquad v=\tilde{v}(x,y,t)Z(z)$$

we obtain

$$(4.1.3) \qquad \frac{d}{dz}\left[\frac{1}{g\Gamma}\left(\frac{dZ}{dz}+\Gamma Z\right)\right]+\nu Z=0$$

and

$$(4.1.4) \qquad \frac{\partial\tilde{P}}{\partial t}+\frac{1}{\nu}\left(\frac{\partial\tilde{u}}{\partial x}+\frac{\partial\tilde{v}}{\partial y}\right)=0.$$

Equ. (4.1.4) is the spectral equation; equ. (4.1.3) together with appropriate boundary conditions defines the eigenvalue problem. (4.1.3) contains the barotropic and the baroclinic modes if the boundary condition is applied at the free sea surface. In this case one obtains a complicated boundary value problem. The problem is considerably simplified - without any notable loss of accuracy - if the barotropic and the baroclinic modes are treated separately. We follow this standard approach where (4.1.3) is only used to describe the baroclinic modes. The boundary conditions in this case are derived from $w = 0$ at $z = 0$ and $z = H$. Due to (2.3.3), we have

$$(4.1.5) \qquad \tilde{w} = -\frac{\partial \tilde{P}}{\partial t} \qquad W(z) = \frac{1}{g\Gamma}\left(\frac{dZ}{dz} + \Gamma Z\right).$$

Thus, the boundary conditions to (4.1.3) are

$$(4.1.6) \qquad \frac{1}{g\Gamma}\left(\frac{dZ}{dz} + \Gamma Z\right) = 0 \qquad \text{for } z = 0 \quad \text{and } z = H.$$

The problem is identical with the well-known equation

$$(4.1.7) \qquad \frac{d^2W}{dz^2} + \Gamma \frac{dW}{dz} + g\Gamma\nu W = 0, \qquad W = 0 \quad \text{for } z = 0 \quad \text{and } z = H.$$

This can be shown as follows: Inserting (4.1.5) into (4.1.3) yields

$$\frac{dW}{dz} + \nu Z = 0 \qquad \text{or} \qquad \frac{d^2W}{dz^2} + \nu \frac{dZ}{dz} = 0.$$

Substituting again (4.1.5) for dZ/dz and replacing Z by $(1/\nu)dW/dz$, we obtain (4.1.7).

The solutions to (4.1.3) subject to (4.1.6) are an orthogonal set of eigenfunctions $Z_n(z)$. The orthogonality relation is

$$(4.1.8) \qquad \int_0^H \bar{\rho}\, Z_n Z_m \, dz = \begin{cases} 0 & \text{for } n \neq m \\ q_n & \text{for } n = m \end{cases}$$

where

$$(4.1.9) \qquad \int_0^H \bar{\rho}\, Z_n^2 \, dz = q_n$$ is the square norm of the eigenfunction.

Any function $Q(z)$ which behaves appropriate to the boundary conditions (4.1.6) may be expanded into eigenfunctions,

$$(4.1.10) \qquad Q(z) = \sum_{n=1}^{\infty} A_n Z_n(z)$$

where the expansion coefficients A_n are given by

$$(4.1.11) \qquad A_n = \frac{1}{q_n} \int_0^H \bar{\rho}\, Q\, Z_n dz.$$

4.2. Equations for free waves: barotropic mode

The barotropic mode is not influenced by the density field. Thus, we can replace (2.2.3) and (2.2.4) by the static equation

$$(4.2.1) \qquad P = g(z + \zeta).$$

Furthermore, (2.2.16) is used in its original form,

$$(4.2.2) \qquad \frac{\partial w}{\partial z} - \Delta\phi = 0.$$

Thus, the system of equations is:

$$(4.2.3) \quad -\frac{\partial}{\partial t}\Delta\phi + \beta\frac{\partial\phi}{\partial x} + \frac{\partial}{\partial z}\left(\mu\frac{\partial\Delta\phi}{\partial z}\right) - \left(f_o\Delta\psi + \beta\frac{\partial\psi}{\partial y}\right) + \Delta P = 0$$

$$(4.2.4) \quad -\frac{\partial}{\partial t}\Delta\psi + \beta\frac{\partial\psi}{\partial x} + \frac{\partial}{\partial z}\left(\mu\frac{\partial\Delta\psi}{\partial z}\right) + f_o\Delta\phi + \beta\frac{\partial\phi}{\partial y} = 0$$

$$(4.2.5) \quad \frac{\partial w}{\partial z} - \Delta\phi = 0$$

Applying

$$(4.2.6) \qquad \bar{\chi} = \frac{1}{H}\int_o^H \chi \, dz$$

and the boundary condition for free waves

$$(4.2.7) \quad \frac{\partial\phi}{\partial z} = \frac{\partial\psi}{\partial z} = 0 \;, \quad w = -\frac{\partial\zeta}{\partial t} = -\frac{1}{g}\frac{\partial P}{\partial t} \qquad \text{at } z = 0$$

$$(4.2.8) \quad \frac{\partial\phi}{\partial z} = -r\bar{\phi} \qquad \frac{\partial\psi}{\partial z} = -r\bar{\psi} \qquad w = 0 \quad \text{at } z = H$$

we arrive at

$$(4.2.9) \quad -\frac{\partial}{\partial t}\Delta\bar{\phi} + \beta\frac{\partial\bar{\phi}}{\partial x} - K_H\Delta\bar{\phi} - \left(f_o\Delta\bar{\psi} + \beta\frac{\partial\bar{\psi}}{\partial y}\right) + \Delta\bar{P} = 0$$

$$(4.2.10) \quad -\frac{\partial}{\partial t}\Delta\bar{\psi} + \beta\frac{\partial\bar{\psi}}{\partial x} - K_H\Delta\bar{\psi} + f_o\Delta\bar{\phi} + \beta\frac{\partial\bar{\phi}}{\partial y} = 0$$

$$(4.2.11) \quad \nu_o\frac{\partial\bar{P}}{\partial t} - \Delta\bar{\phi} = 0$$

where P has been replaced by $\bar{P}$ in (4.2.11). This is allowed because the barotropic pressure at $z = 0$ is identical with the vertically averaged one.

Furthermore, we use

$$(4.2.12) \qquad K_H = \frac{\mu(H)r}{H} \qquad\qquad \nu_o = \frac{1}{gH}$$

Note, that in (4.2.8) $\partial\psi/\partial z$ is supposed to be proportional to the mean current, not to the bottom current which may be reduced within the frictional layer.

4.3. Equations for free waves; baroclinic modes

As mentioned above, the treatment of the viscous term in the baroclinic equations poses some problems. This can best be elucidated by starting from the initial set of equations (2.2.1), (2.2.2) and (4.1.1).

From

$$(4.3.1) \quad u = \sum_{m=1}^{\infty} \hat{u}_m(x,y,t)Z_n(z), \quad v = \sum_{m=1}^{\infty} \tilde{v}_m(x,y,t)Z_n(z), \quad P = \sum_{m=1}^{\infty} \tilde{P}_m(x,y,t)Z_n(z)$$

we obtain for the first two equations

$$(4.3.2)\quad \sum_m \left\{ \frac{\partial \tilde{u}_m}{\partial t} + (f_o + \beta y)\, \tilde{v}_m + \frac{\partial \tilde{P}_m}{\partial x} \right\} Z_m - \frac{\partial}{\partial z}\left(\mu \frac{\partial u}{\partial z}\right) = 0$$

$$(4.3.3)\quad \sum_m \left\{ \frac{\partial \tilde{v}_m}{\partial t} - (f_o + \beta y)\, \tilde{u}_m + \frac{\partial \tilde{P}_m}{\partial y} \right\} Z_m - \frac{\partial}{\partial z}\left(\mu \frac{\partial v}{\partial z}\right) = 0$$

Multiplying by $\bar{\rho}\, Z_n$, integrating over the entire range $[0,H]$, and taking into account the orthogonality relation (4.1.8), we obtain

$$(4.3.4)\quad \frac{\partial \hat{u}_n}{\partial t} + (f_o + \beta y)\, \tilde{v}_n + \frac{\partial \hat{P}_n}{\partial x} - \frac{1}{q_n} \int_o^H \frac{\partial}{\partial z}\left(\mu \frac{\partial u}{\partial z}\right) \bar{\rho}\, Z_n dz = 0$$

$$(4.3.5)\quad \frac{\partial \tilde{v}_n}{\partial t} - (f_o + \beta y)\, \tilde{u}_n + \frac{\partial \tilde{P}_n}{\partial y} - \frac{1}{q_n} \int_o^H \frac{\partial}{\partial z}\left(\mu \frac{\partial v}{\partial z}\right) \bar{\rho}\, Z_n dz = 0$$

These equations show that the viscous term is, in general, not separable. Separability is only achieved if we assume $\mu = \mu_o/\Gamma$ and if we neglect ΓZ in (4.1.3). The latter is no restriction. In this case we have - by virtue of (4.1.3)

$$\int_o^H \frac{\partial}{\partial z}\left(\mu \frac{\partial u}{\partial z}\right) \bar{\rho}\, Z_n dz = \int_o^H \sum_m \tilde{u}_m \mu_o \frac{\partial}{\partial z}\left(\frac{1}{\Gamma} \frac{dZ_m}{dz}\right) \bar{\rho}\, Z_n \qquad (4.3.6)$$

$$= -\sum_m \tilde{u}_m\, g\, \mu_o\, \nu_m \int_o^H \bar{\rho} Z_n Z_m\, dz = -\, g\, \mu_o\, \nu_n \hat{u}_n q_n .$$

However, the inverse proportionality between μ and Γ - which has been used e.g. by J.E. Fjeldstad (1964) and M. Mork (1968) - gives very unrealistic high eddy viscosities in the deep ocean

where Γ approaches zero. We prefer to approximate the viscous term in the baroclinic case similarly to that in the barotropic case. For this purpose, we recall that for the barotropic mode the entire energy dissipation is due to bottom friction,

$$(4.3.7) \qquad E_{Diss} = \tilde{u}\ (-\mu\ \frac{\partial u}{\partial z})_H = \mu\ r\ \tilde{u}^2 = K_H H \tilde{u}^2$$

In the baroclinic case we additionally have a contribution from internal dissipation. By means of partial integration of the last term of (4.3.4) and $\frac{\partial u}{\partial z}\Big|_o = 0$, we obtain

$$(4.3.8) \qquad -\frac{1}{q_n \tilde{u}_n} \int_o^H \frac{\partial}{\partial z} (\mu\ \frac{\partial u}{\partial z})\ \rho \tilde{u}_n Z_n dz = -\Big[\frac{1}{\tilde{u}_n q_n}\ \rho \tilde{u}_n Z_n\ \mu\ \frac{\partial u}{\partial z}\Big|_H$$

$$+ \frac{1}{\tilde{u}_n q_n} \int_o^H \frac{\partial}{\partial z}\ (\rho\ u_n Z_n)\ \mu\ \frac{\partial u}{\partial z}\ dz$$

where the first term on the right-hand side resembles the contribution of mode n to the energy dissipation at the bottom and the second one in the interior of the water column. Its contribution is, in general, small compared to bottom friction and will be neglected.

With respect to bottom friction, we assume that each mode contributes the same amount to the total dissipation as does the barotropic one if their vertically averaged energy is the same.

The energy dissipation of mode n at the bottom is $-(\tilde{u}_n Z_n \mu \partial u/\partial z)_H$. In order to make it equal to that of the barotropic mode, equ. (4.3.7), we must require

$$(4.3.9)\quad E_{Diss} = \left[\hat{u}_n Z_n \left(-\mu \frac{\partial u}{\partial z}\right)\right]_H = K_H H \frac{1}{H} \int_0^H \hat{u}_n^2 Z_n^2 dz \,.$$

The bottom friction in (4.3.8) then takes the form

$$(4.3.10)\quad -\left| \frac{1}{\tilde{u}_n q_n} \bar{\rho}\, \hat{u}_n Z_n \mu \frac{\partial u}{\partial z} \right|_H = K_H \tilde{u}_n \frac{\bar{\rho} \int_0^H Z_n^2 dz}{\int_0^H \bar{\rho} Z_n^2 dz} \approx K_H \tilde{u}_n \,.$$

The equations for the baroclinic modes then read

$$(4.3.11)\quad \frac{\partial \hat{u}_n}{\partial t} + (f_o + \beta y)\tilde{v}_n + K_H \tilde{u}_n + \frac{\partial \hat{P}_n}{\partial x} = 0$$

$$(4.3.12)\quad \frac{\partial \hat{v}_n}{\partial t} - (f_o + \beta y)\,\tilde{u} + K_H \tilde{v}_n + \frac{\partial \hat{P}_n}{\partial y} = 0 \,.$$

Introducing divergence and vorticity, the final equations are

$$(4.3.13)\quad -\frac{\partial}{\partial t} \Delta\hat{\phi}_n + \beta \frac{\partial \hat{\phi}_n}{\partial x} - K_H \Delta\hat{\phi}_n - \left(f_o \Delta\tilde{\psi}_n + \beta \frac{\partial \tilde{\psi}_n}{\partial y}\right) + \Delta\hat{P}_n = 0$$

$$(4.3.14) \qquad -\frac{\partial}{\partial t}\Delta\tilde{\psi}_n + \beta\frac{\partial\tilde{\psi}_n}{\partial x} - K_H\Delta\tilde{\psi}_n + f_o\Delta\tilde{\phi}_n + \beta\frac{\partial\tilde{\phi}_n}{\partial y} = 0$$

$$(4.3.15) \qquad \nu_n\frac{\partial\tilde{P}_n}{\partial t} - \Delta\phi_n = 0$$

where the last equation results from (4.3.1) by virtue of (4.1.3).

The system (4.3.13) - (4.3.15) is identical with (4.2.9) - (4.2.11) if the proper eigenvalue is chosen. All modes, therefore, can be treated the same way.

4.4. Equations in the Fourier space

If we replace $\Delta\tilde{\phi}_n$ in (4.3.15) and (4.3.16) by means of (4.3.17), Fourier transformation with respect to y and t yields

$$(4.4.1) \qquad \frac{d^2\hat{P}_n}{dx^2} - (\eta^2 - \omega^2\nu_n + i\omega\nu_n K_H)\hat{P}_n - f_o\frac{d^2\hat{\psi}_n}{dx^2} + (f_o\eta^2 - i\beta\eta)\hat{\psi}_n + \beta\frac{d\hat{\phi}_n}{dx} = 0$$

$$(4.4.2) \qquad (i\omega+K_H)\frac{d^2\hat{\psi}_n}{dx^2} - \eta^2(i\omega+K_H)\hat{\psi}_n - \beta\frac{d\hat{\psi}_n}{dx} - i\omega\nu_n f_o\hat{P}_n - i\beta\eta\hat{\phi}_n = 0$$

$$(4.4.3) \qquad \frac{d^2\hat{\phi}_n}{dx^2} - \eta^2\hat{\phi}_n - i\omega\nu_n\hat{P}_n = 0$$

which - in real form - and ordered according to the second derivatives of ϕ, ψ, and P, read:

$$
(4.4.4)\quad \begin{cases}
\dfrac{d^2\tilde{\phi}_{n1,2}}{dx^2} - \eta^2\tilde{\phi}_{n1,2} + \omega\nu_n \tilde{P}_{n2,1} = 0 \\[2ex]
\dfrac{d^2\tilde{\psi}_{n1,2}}{dx^2} - \dfrac{\beta K_H}{D}\dfrac{d^2\tilde{\psi}_{n1,2}}{dx} \mp \dfrac{\beta\omega}{D}\dfrac{d\tilde{\psi}_{n2,1}}{dx} - \eta^2\,\tilde{\psi}_{n1,2} - \dfrac{\omega^2\nu_n f_o}{D}\tilde{P}_{n1,2} \\[2ex]
\qquad \pm \dfrac{\omega K_H f_o \nu_n}{D}\tilde{P}_{n2,1} - \dfrac{\beta\eta\omega}{D}\tilde{\phi}_{n1,2} \pm \dfrac{\beta\eta K_H}{D}\tilde{\phi}_{n2,1} = 0 \\[2ex]
\dfrac{d^2\tilde{P}_{n1,2}}{dx^2} - (\eta^2-\omega^2\nu_n)\,\tilde{P}_{n1,2} \pm \omega\nu_n K_H \tilde{P}_{n2,1} - f_o\dfrac{d^2\tilde{\psi}_{n1,2}}{dx^2} + f_o\eta^2\,\tilde{\psi}_{n1,2} \\[2ex]
\qquad \pm \beta\eta\,\tilde{\psi}_{n2,1} + \dfrac{\beta d\tilde{\phi}_{n1,2}}{dx} = 0
\end{cases}
$$

where

$$
(4.4.5)\qquad D = \omega^2 + K_H^2
$$

The system (4.4.4) is to be integrated numerically with respect to x.

4.5. The horizontal boundary conditions for a rectangular basin of constant depth

The boundary conditions must be fulfilled by the sum of free and forced solutions. This sum is denoted by a hut, i.e. $\hat{\psi}$. For what follows, we assume that the forced solution has been expanded into eigenfunctions already (section 4.6).

According to section 2.3 the rectangular domain is considered to be open at y = 0 and y = Y. At the rigid walls x = 0 and x = X the kinematic boundary condition requires vanishing velocities in normal direction, (2.3.7), which in the Fourier domain η, ω reads

$$(4.5.1) \qquad \hat{u}_n = -\frac{d\hat{\phi}_n}{dx} + in\,\hat{\psi}_n = 0 \qquad \text{at } x = 0, \quad x = X.$$

Due to the introduction of the stream function ψ and the velocity potential ϕ, however, we raised the order of the system of differential equations with respect to x and y - system (4.4.1) through (4.4.3) -. Instead of having a second-order system with respect to x, we raised the system to sixth order which requires two additional conditions at each side. These are obtained from the original equations of motion in the form (4.3.11) and (4.3.12) by neglecting the β-term.

If we denote the free solutions by $\hat{u}_n$, the forced ones by $\mathring{u}_n$ (and similarly for $\hat{v}_n$ and $\hat{P}_n$), then the combination of

$$\hat{u}_n = \hat{u}_n + \mathring{u}_n = 0 \tag{4.5.2}$$

and

$$\begin{cases} \dfrac{\partial \tilde{u}_n}{\partial t} + f\tilde{v}_n + K_H \tilde{u}_n + \dfrac{\partial \tilde{P}_n}{\partial x} = 0 \\ \dfrac{\partial \tilde{v}_n}{\partial t} - f\tilde{u}_n + K_H \tilde{v}_n + \dfrac{\partial \tilde{P}_n}{\partial y} = 0 \end{cases} \tag{4.5.3}$$

yields

$$\begin{cases} \dfrac{d\hat{\phi}_n}{dx} - in\hat{\psi}_n = -\left(\dfrac{d\mathring{\phi}_n}{dx} - in\mathring{\psi}_n\right) \\ \dfrac{d\hat{\psi}_n}{dx} + in\hat{\phi}_n + \dfrac{in(i\omega - K_H)}{D}\hat{P}_n = \dfrac{f(i\omega - K_H)}{D}\left(\dfrac{d\mathring{\phi}}{dx} - in\mathring{\psi}_n\right) \\ \dfrac{d\hat{P}_n}{dx} + \dfrac{ifn(i\omega - K_H)}{D}\hat{P}_n = -(i\omega + K_H - \dfrac{f^2(i\omega - K_H)}{D}\left(\dfrac{d\mathring{\phi}_n}{dx} - in\mathring{\psi}_n\right) \end{cases} \tag{4.5.4}$$

where $\tilde{u}_n$ in (4.5.3) has been replaced by $-\mathring{u}_n$ according to (4.5.2).

Real and imaginary parts are then given by

$$\frac{d\tilde{\phi}_{n1,2}}{dx} \pm n\,\tilde{\psi}_{n2,1} = -\left(\frac{d\tilde{\phi}_{n1,2}}{dx} \pm n\,\tilde{\psi}_{n2,1}\right) = -D_{n1,2}$$

$$\frac{d\tilde{\psi}_{n1,2}}{dx} \mp n\tilde{\phi}_{n2,1} - \frac{\omega n}{D}\tilde{P}_{n1,2} \pm \frac{nK_H}{D}\tilde{P}_{n2,1} = -\frac{f_o K_H}{D} D_{n1,2} \mp \frac{f_o \omega}{D} D_{n2,1} \qquad (4.5.5)$$

$$\frac{d\tilde{P}_{n1,2}}{dx} - \frac{n\omega f_o}{D}\tilde{P}_{n1,2} \pm \frac{nf_o K_H}{D}\tilde{P}_{n2,1} = -\frac{K_H(f_o^2+D)}{D} D_{n1,2} \mp \frac{\omega(f_o^2-D)}{D} D_{n2,1}$$

$D_{n1,2}$ are the mode amplitudes of D_1, D_2, which are given at $x = 0$ by

$$(4.5.6) \qquad D_{1,2}(0,z,\eta,\omega) = \frac{d\hat{\phi}_{1,2}(0,z,\eta,\omega)}{dx} \pm \eta\psi_{2,1}(0,z,\eta,\omega)$$

The relation between D_i and $D_{i,n}$ is

$$(4.5.7) \qquad D_i(0,z,\eta,\omega) = \sum_{n=0}^{N} D_{i,n}(0,\eta,\omega)\, Z_n(z) \qquad (i = 1,2)$$

where

$$(4.5.8) \qquad D_{i,n}(0,\eta,\omega) = \frac{1}{q_n} \int_0^H \bar{\rho} D_i(0,z,\eta,\omega)\, Z_n(z)dz \,.$$

The wind field is a periodic function with period 2X.

Consequently

$$(4.5.9) \qquad D_i(X,\eta,\omega,z) = - D_i(0,\eta,\omega,z)$$

5. The final set of equations

For convenience, we summarize the equations required for the numerical model.

5.1. The forcing functions

Wind stress $\tau^{(x)}$, $\tau^{(y)}$ and air pressure P_o have to be expanded into a Fourier-series according to (2.4.1) or (2.4.10).

The stress field $\tau^{(x)}$ should be expanded into an odd function with respect to x and into an even function with respect to y. $\tau^{(y)}$ is even in x and y.

5.2. The forced solution

The system (2.4.11) subject to the boundary conditions (2.4.12) and (2.4.13) has to be integrated numerically with respect to z for each ω_m, κ_k, η_ℓ -combination where $1 \leq m \leq M$, $-K \leq k \leq K$, $-L \leq \ell \leq L$, except $k=0$ and $\ell=0$. The final solution is given by sums according to (2.4.10). Γ and μ are prescribed functions of z.

5.3. The horizontal boundary conditions

In order to apply the boundary conditions at x = 0 and x = X, the forced solution (4.5.6 has to be expanded according to (4.5.7) - (4.5.9) into eigenfunctions.

5.4. The free solution

These solutions are obtained by numerical integration of (4.4.4.) with respect to x subject to the boundary conditions

(4.5.5) for each ω,η-combination. The solutions are summed up according to (2.4.10).

5.5. The total solution

The final solution for ψ,ϕ and P is obtained by summation of the free and the forced solutions. u and v are derived according to (2.2.12). The vertical velocity can be obtained from P according to (2.3.3), the density field from (2.2.4) and $\bar{\rho}$.

Details of the numerical procedure and examples are given in part 2.

REFERENCES

BRYAN, K., 1963: A numerical investigation of a nonlinear model of a wind-driven ocean.
J. Atmos. Sci. 20, 594-602

BRYAN, K., 1969: A numerical method for the study of ocean circulation.
J. Comp. Phys. 4, 347-376

CHARNEY, J.G. & G.R. FLIERL, 1981: Oceanic analogues of large-scale atmospheric motions. In: Evolution of Physical Oceanography (edit. by B.A. Warren & C. Wunsch).
MIT Press, 504-548

DAVIS, A.M., 1979: Application of numerical models to the computation of the wind-induced circulation of the North Sea during JONSDAP 76.
METEOR-Forsch.Erg., Ser. A.

FJELDSTAD, J.E., 1964: Internal waves of tidal origin.
Geof. Publ. 25, 5

HAIDVOGEL, D.B., A.R. ROBINSON & F.F. SCHULMAN, 1980: The accuracy, efficiency and stability of three numerical models with application to open ocean problems.
J. Comp. Phys., 34, 1-53

HANSEN, W., 1956: Theorie zur Errechnung des Wasserstandes und der Strömungen in Randmeeren nebst Anwendungen.
TELLUS 8, 287-300

HEAPS, N.S., 1972: On the numerical solution of the three-dimensional hydrodynamical equations for tides and storm surges.
Mem. Soc. R. Sci., Liège Ser. 6 (2), 143-180

HOLLAND, W.R. & L.B. LIN, 1975: On the generation of mesoscale eddies and their interaction with the oceanic general circulation. Part 1 and 2. J. Phys. Oceanogr. 5, 462-669

KRAUSS, W., 1966: Interne Wellen.
Borntraeger-Verlag, Berlin, 248 pp.

KRAUSS, W., 1976: On currents, internal and inertial waves in a stratified ocean due to variable winds. Part 1.
Dtsch. Hydrogr. Z., 29, 87-96

KRAUSS, W., 1979: A semi-spectral model for the computation of mesoscale processes in a stratified channel of variable depth. Dtsch. Hydrogr. Z., 32, 173-189

KRAUSS, W. & Chr. WÜBBER, 1982: The response of the North Atlantic to annual wind variations along the eastern coast. Deep-Sea Res., 29, No. 7A, 851-868

LeBLOND, P.H. & I.A. MYSAK, 1977: Waves in the ocean. Elsevier, Amsterdam, 602 pp.

MACHENHAUER, B., 1979: The spectral method. Numerical methods used in atmospheric models., Chapter 3. GARP Publ. Series No. 17, Part 2, 124-275

MORK, M., 1968: The response of a stratified sea to atmospheric forces. Universitetet i Bergen. Geofisisk Institutt, 30 pp.

SIMONS, T.J., 1973: Development of three-dimensional numerical models of the Great Lakes. Can. Inland Waters Branch, Sci. Ser. 12, 26 p.

STOMMEL, H., 1948: The westward intensification of wind-driven ocean currents. Trans. Amer. Geophys. Union, 29, 202-206

VERONIS, G. & H. STOMMEL, 1956: The action of variable wind stresses on a stratified ocean. J. Mar. Res. 15, 43-75

WILLEBRAND, J., S.G.H. PHILANDER & R.C. PACANOWSKI, 1978: The ocean response to large-scale atmospheric disturbances. J. Phys. Oceanogr. 10, 411-429

YOUNG, W.R., 1981: The vertical structure of the wind-driven circulation. Ph. D. Thesis. Mass. Inst. of Techn. / WHOI, WHOI-81-89

List of symbols

If not explained in the text the symbols have the following meaning:

D	divergence
$f = f_o + \beta y$	Coriolis parameter
H	depth
$k^2 = \kappa^2 + \eta^2$	
K_H	bottom friction of each mode
p	pressure
$P = \frac{p}{\bar{\rho}}$	reduced pressure
P_o	air pressure
q	square norm of eigenfunction
$R = \frac{\rho}{\bar{\rho}}$	reduced density
r	bottom friction
t	time
u, v, w	velocity components in x, y, z, respectively
x	east west coordinate, $0 \leq x \leq X$, positive eastwards
y	north south coordinate, $0 \leq y \leq Y$, positive northwards
z	vertical coordinate, $0 \leq z \leq H$, positive downwards
Z	eigenfunctions (equ. 4.1.3)
$\beta = df/dy$	
$\Gamma = \frac{1}{\bar{\rho}} \frac{d\bar{\rho}}{dz}$	stability parameter, $\Gamma' = d\Gamma/dz$
ζ	surface elevation
κ, η	wave numbers with respect to x, y

μ	eddy viscosity, $\mu' = d\mu/dz$
ν	eigenvalue
ξ	vorticity
ρ	density
$\bar{\rho}(z)$	mean density
$\tau^{(x)}$, $\tau^{(y)}$	windstress components
ϕ	velocity potential (equ. 2.2.12)
$\tilde{\chi}$	complex Fourier amplitude $\tilde{\chi} = \chi_1 + i\chi_2$ in section 2.4; real or complex amplitude of the free waves in the mode decomposition, otherwise,
$\bar{\chi}$	barotropic part of χ (equ. 4.2.6)
$\overset{\circ}{\chi}$	forced solution of χ
ψ	stream function (equ. 2.2.12)
ω	frequency

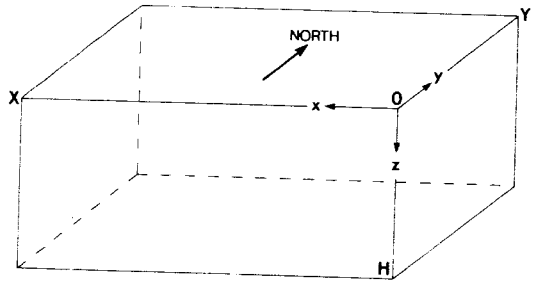

Fig. 1: Coordinate System and Basis
Part 1

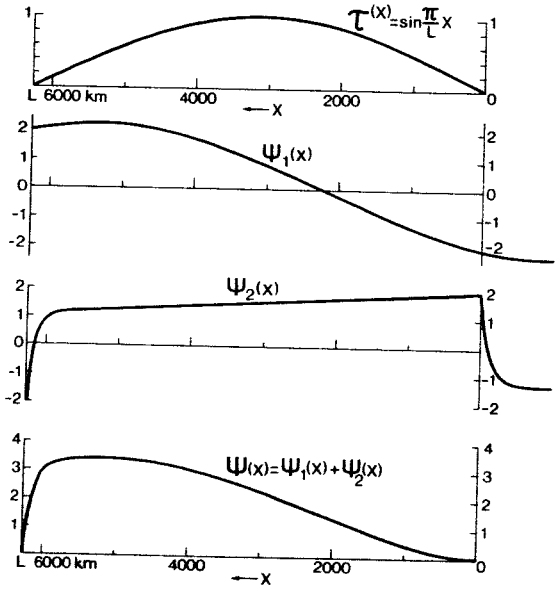

Fig. 2: Forced and free solution to the Stommel problem
Part 1 (τ in dyne and ψ in arbitrary units, depending on H)

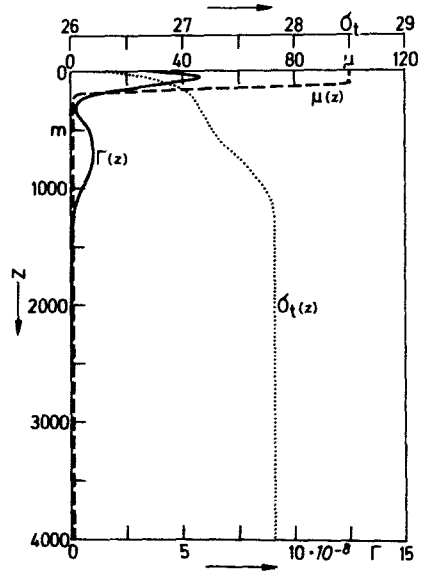

Fig. 3: Part 1 — Mean density, stability and eddy viscosity used in the model (Γ and μ in cgs-units)

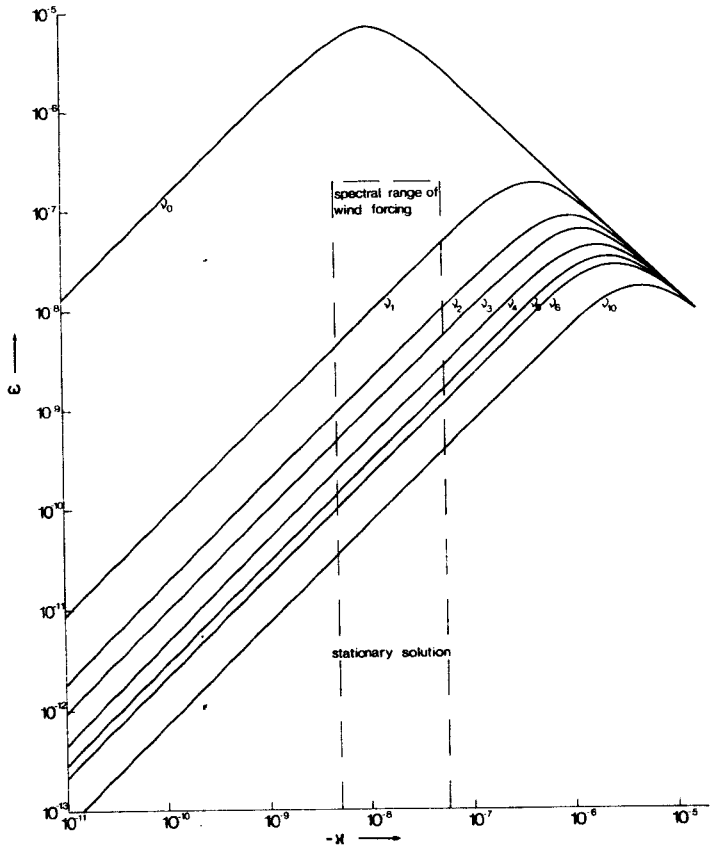

Fig. 4: Part 1

Dispersion curves for barotropic (ν_o) and baroclinic (ν_1 - ν_{10}) Rossby waves

PART 2:

NUMERICAL SCHEMES AND EXAMPLES

Summary:

The numerical procedures used in solving the linear hydrodynamic equations on the ß-plane are being described. The response characteristics of a rectangular ocean basin are discussed and examples of the solution given. For a vertical resolution of 20 m and a horizontal one (x-direction) of 30 km, the model needs only 60 sec computer time per frequency and meridional wave number on a CYBER 76. In the present form it can be applied to the frequency ranges of baroclinic and barotropic Rossby waves.

Zusammenfassung:

Es wird ein numerisches Verfahren zur Lösung des linearisierten hydrodynamischen Gleichungssystems auf der ß-Ebene angegeben. Anschliessend wird die Reaktion eines rechteckigen Ozeans auf variable Windfelder behandelt und anhand von Beispielen erläutert.

Das Modell benötigt pro Frequenz und meridionaler Wellenzahl bei einer Vertikalauflösung von 20m und einer Horizontalauflösung in x-Richtung von 30 km nur 60 sec Rechenzeit auf einer CYBER 76. Der Anwendungsbereich des Modelles liegt im Frequenzbereich der barotropen und baroklinen Rossby-Wellen.

1. Introduction

In Part 1 of this paper (which will be cited as I in the following), we outlined the general characteristics of a recently developed numerical model of the wind-driven circulation on a ß-plane. The model should allow high vertical resolution in order to gain more insight into the vertical structure of the processes which occur. Furthermore, horizontal and time derivatives should be approximated as accurately as possible. In order to meet these requirements the solutions are decomposed into a forced and a free solution. The forced solution is the response of an infinite ß-plane ocean to the meteorological forces. It is obtained by Fourier decomposition of the forces with respect to the horizontal coordinates and time, and numerical integration with respect to depth. This procedure allows solutions for arbitrary density distributions and eddy viscosities with respect to the vertical coordinate.
In order to fulfill the horizontal boundary conditions along the coasts, we have to add a free solution of the system with homogeneous boundary conditions at $z = 0$. The dominating signal in this solution is the western boundary current which resembles many features of a δ-function. Because the spectrum of a δ-function is white,

we compute the free solution by numerical integration with respect to the East-West coordinate and use Fourier series in y and t. The vertical dependency of this solution is decomposed into eigenfunctions and fitted to the forced solution at the horizontal boundaries. The

sum of both solutions, the forced and the free one, meets all boundary conditions.

Alternative to the phrases "forced" and "free" solution, we could use the term "Green's function". In order to obtain the forced solution, we could construct the Green's function of the meteorological forces and that of the boundary condition. At any point in the interior the entire solution is given by the contributions from both.

In its present version the model is linear and applied to a rectangular box with solid walls in North-South direction. The model is periodic with respect to y. The incorporation of bottom topography, arbitrary coast lines and non-linear terms is beyond the scope of the present paper.

2. Numerical treatment of the equations

The system of equations which has to be solved, was summarized in I, section 5. We now refer to these equations.

2.1. Spectra of the forcing functions

The most important driving force for the general circulation in the ocean is the vorticity of the windstress. According to I, it must be Fourier-expanded for the model. As $\tau^{(x)} = \tau_o \cos \frac{\pi}{Y} y$ is a rather good approximation to the mean wind field in low and mid-latitudes, we need only

a few harmonics, if $\tau^{(x)}$ is expanded according to $\cos \pi y/Y$, where Y is the meridional extension of the basin.

Similarly, $\tau^{(y)} = -\tau_o \cos(\pi x/X) \cos(\pi y/Y)$ is a first approximation to the meridional component suggesting an expansion like this one.

Another aspect is that the vorticity of the wind field in such an expansion becomes zero at the borders. If we would use the area $0 \leq x \leq X$, $0 \leq y \leq Y$ as the basic domain of the periodic functions, we would introduce strong shear zones at the borders. We thus use the following expansions (Fig. 1).

Let the time series of the forcing function $F(x,y,t)$ be given at the points $x = k\Delta x$, $y = \ell\Delta y$ in the interior of the basin $0 < x < X$, $0 < y < Y$, at its rigid walls $x = 0$ and $x = X$ and at its open boundaries $y = 0$ and $y = Y$ for the time range $0 \leq t \leq 2T$ where $2T$ is the basic period, and $0 \leq k \leq 2K$, $0 \leq \ell \leq 2L$.

The fields are then extrapolated over the domain $X \leq x \leq 2X$, $Y < y < 2Y$ in the following manner:-

i) $\tau^{(x)}$ is continued as odd function with respect to x and even function with respect to y. For arbitrary wind fields the Fourier component $\tau^{(x)}(0,\eta,\omega) = 0$ due to oddness with respect to x. To ensure also $\tau^{(x)}(\kappa,0,\omega)=0$, we subtract the mean values

$$\tau^{(x)}_m = \frac{1}{2Y+1} \sum_{\ell=0}^{2L} \tau^{(x)}(\kappa,\ell\Delta y,t)$$

ii) $\tau^{(y)}$ is continued as even function with respect to x and y. To obtain $\tau^{(y)}(0,\eta,\omega) = 0$ and $\tau^{(y)}(\kappa,0,\omega)=0$ we subtract the mean values

$$\tau^{(y)}_{m_1} = \frac{1}{2K+1} \sum_{k=0}^{2K} \tau^{(y)}(k\Delta x,\ell,t) \quad \text{and} \quad \tau^{(y)}_{m_2} = \frac{1}{2L+1} \sum_{\ell=0}^{2L} \tau^{(y)}(k,\ell\Delta y,t).$$

iii) As the air pressure P_o acts directly on the pressure field (no derivatives are involved), no precaution is required for the continuation of this field. However, the mean values

$$P_{o,m_1} = \frac{1}{2K+1} \sum_{k=0}^{2K} P_o(k\Delta x,\ell,t) \quad \text{and} \quad P_{o,m_2} = \frac{1}{2L+1} \sum_{\ell=0}^{2L} P_o(k,\ell\Delta y,t)$$

are again subtracted for reasons outlined below.

The Fourier expansion of the fields thus obtained, is

$$(2.1.1) \qquad F(x,y,t) = 2 \sum_{m=1}^{M} \sum_{k=-K}^{K} \sum_{\ell=-L}^{L} F(k,\ell,m)\, e^{i(k\kappa_o x+\ell\eta_o y + m\omega_o t)}$$

where

$$(2.1.2) \qquad \kappa_o = \frac{\pi}{X}, \qquad \eta_o = \frac{\pi}{Y}, \qquad \omega_o = \frac{\pi}{T}$$

and

$$(2.1.3) \qquad F(k,\ell,m) = \frac{1}{XYT} \sum_{m=1}^{M} \sum_{k=-K}^{K} \sum_{\ell=-L}^{L} F(k\Delta x,\ell\Delta y,m\Delta t) e^{-i(k\kappa_o x+\ell\eta_o y+m\omega_o t)}$$

$$(2.1.4) \qquad F(o,\ell,m) = F(k,o,m) = 0$$

The summation with respect to m is over the positive range only due to the reality condition of F.

The mean values have been subtracted in order to exclude $\kappa = 0$ and $\eta = 0$ which would destroy the geostrophic balance in the oceanic response. The mean values are included into the calculation by an odd expansion (Fig. 2) and subsequent Lanczos filtering (GODIN, 1972),

$$(2.1.5) \qquad 1 = \sum_{\substack{\ell=1 \\ \text{odd}}}^{L} \left(\frac{L}{\ell^2 \pi} \sin \frac{\ell\pi}{L}\right) \sin \ell\eta_o y$$

and similarly with respect to x.

2.2. The forced solution

For arbitrary distributions of $\Gamma(z)$ and $\mu(z)$ the system (I. 2.4.11) - subject to the boundary conditions (I.2.4.12-13) - can only be solved numerically. Using central differences

$$(2.2.1) \qquad \frac{d\psi}{dz} \to \frac{\psi(n+1)-\psi(n-1)}{2\Delta z} \qquad \frac{d^2\psi}{dz^2} \to \frac{\psi(n+1)-2\psi(n)+\psi(n-1)}{(\Delta z)^2}$$

the system (I.2.4.11) may be written in Matrix form as

$$(2.2.2) \qquad A(n)\cdot\vec{U}(n+1) + B(n)\cdot\vec{U}(n) + C(n)\cdot\vec{U}(n-1) = 0 \text{ for } n=1,2,..,N-1$$

where the range $0 \leq z \leq H$ has been discretisized according to

$$(2.2.3) \qquad z = n\Delta z, \qquad n = 0, 1, \ldots, N.$$

Typically, Δz is 20 m. The column vector $\vec{U}$ is defined by

$$(2.2.4) \qquad \vec{U} = (\phi_1, \phi_2, \psi_1, \psi_2, P_1, P_2)$$

and the 6×6 matrices by

$$(2.2.5) \qquad A(n) = a_1^+ I$$

$$(2.2.6) \quad B(n) = \begin{pmatrix} -(2s+\frac{Ak^2}{\mu(n)}) & (\frac{\omega}{\mu(n)}+\frac{\kappa\beta}{k^2\mu(n)}) & -\frac{f_o}{\mu(n)} & -\frac{\eta\beta}{k^2\mu(n)} & \frac{1}{\mu(n)} & 0 \\ -(\frac{\omega}{\mu(n)}+\frac{\kappa\beta}{k^2\mu(n)}) & -(2s+\frac{Ak^2}{\mu(n)}) & \frac{\eta\beta}{k^2\mu(n)} & -\frac{f_o}{\mu(n)} & 0 & \frac{1}{\mu(n)} \\ \frac{f_o}{\mu(n)} & \frac{\eta\beta}{k^2\mu(n)} & -(2s+\frac{Ak^2}{\mu(n)}) & (\frac{\omega}{\mu(n)}+\frac{\kappa\beta}{k^2\mu(n)}) & 0 & 0 \\ -\frac{\eta\beta}{k^2\mu(n)} & \frac{f_o}{\mu(n)} & -(\frac{\omega}{\mu(n)}+\frac{\kappa\beta}{k^2\mu(n)}) & -(2s+\frac{Ak^2}{\mu(n)}) & 0 & 0 \\ 0 & -\frac{g\Gamma(n)k^2}{\omega} & 0 & 0 & -2s & 0 \\ \frac{g\Gamma(n)k^2}{\omega} & 0 & 0 & 0 & 0 & -2s \end{pmatrix}$$

(2.2.7) $C(n) = a_1^{\sim} I$

where

(2.2.8) $k^2 = \kappa^2 + \eta^2$, $a_i^{\pm} = s \pm s_1(n)$ for rows 1 to 4 and

$a_i^{\pm} = s_2^{\pm}(n)$ for rows 5 and 6

(2.2.9) $s = \frac{1}{(\Delta z)^2}$ $\quad s_1(n) = \frac{\mu'(n)}{2\mu(n)\Delta z}$

(2.2.10) $s_2^{\pm}(n) = \frac{1}{(\Delta z)^2} \pm \frac{\Gamma(n)}{2\Delta z} \mp \frac{\Gamma'(n)}{\Gamma(n)2\Delta z}$

(Horizontal eddy viscosities A have been included.)

The boundary condition (I.2.4.12) may be written as

(2.2.11) $\vec{U}(1) - \vec{U}(0) = \Delta z \cdot \vec{Q}(0)$

where

(2.2.12) $\vec{Q}(0) = \frac{1}{k^2\mu(0)} \left((\kappa T_2 + \eta T_4), -(\kappa T_1 + \eta T_3), -(\eta T_2 - \kappa T_4), (\eta T_1 - \kappa T_3), \right.$
$\left. - \frac{\Gamma(0)k^2\mu(0)}{\rho(0)} T_5, - \frac{\Gamma(0)k^2\mu(0)}{\rho(0)} T_6 \right)$

At the bottom (I.2.4.13) yields

$$\vec{U}(N) - \vec{U}(N-1) - \Delta z \; M(N) \cdot \vec{U}(N) = 0 \tag{2.2.13}$$

where

$$M(N) = r_i I, \; r_i = r \text{ for rows 1 to 4 and } r_i = -\Gamma(N) \text{ for rows 5 and 6.} \tag{2.2.14}$$

The numerical procedure to solve these equations is based on schemes as described by LINDSEN & KUO (1969), RICHTMYER & MORTON (1967) etc. and has been described in detail by KRAUSS (1976). For convenience, the main steps are summarized below:

Introducing

$$\vec{U}(n) = \alpha(n) \, \vec{U}(n+1) + \vec{\beta}(n) \tag{2.2.15}$$

we obtain from (2.2.2)

$$\begin{aligned} [B(n) + C(n) \cdot \alpha(n-1)] \cdot \alpha(n) &= - A(n) \\ [B(n) + C(n) \cdot \alpha(n-1)] \cdot \vec{\beta}(n) &= - C(n) \cdot \vec{\beta}(n-1) \end{aligned} \tag{2.2.16}$$

which allows to compute $\alpha(n)$, $\vec{\beta}(n)$ inductively in order

of increasing n ($n = 1,2,--,N-1$). At $n = 0$, we have

(2.2.17) $\qquad \alpha(0) = I, \qquad \vec{\beta}(0) = -\Delta z\, \vec{Q}(0)$

The $\vec{U}(n)$ are obtained from the $\alpha(n)$, $\vec{\beta}(n)$, by means of the boundary condition at the bottom (2.2.13) which by means of (2.2.15) is

(2.2.18) $\qquad [I - \alpha(N-1) - \Delta z\, M(N)]\cdot\vec{U}(N) = \vec{\beta}(N-1)$

After computation of $\vec{U}(N)$, (2.2.15) allows to calculate the remaining $\vec{U}(n)$ in decreasing order. Thus, the forced solution is completed.

2.3. Response characteristics

For a baroclinic ocean, we prescribe the stability distribution $\Gamma(z)$ and the eddy viscosity $\mu(z)$. Fig. 3 displays $\Gamma(z)$ according to the mean density distribution in the central North Atlantic (Azores area) and a chosen distribution of μ . For mid-latitudes, $\phi = 45^{o}$, the dispersion relations for barotropic (ν_o) and baroclinic Rossby waves ($\nu_1 - \nu_{1o}$) are displayed in Fig. 4. They have been discussed in part I of this paper.

For a unit wind stress $\tau^{(x)} = \exp\,[i(\kappa x+\eta y+\omega t)]$, where $\eta = 10^{-8}$, the response is shown in Fig. 5 - as function of the wave number κ.

As a measure for the response, we use the kinetic energy of the horizontal currents at the sea surface, $E_{kin}(z=0) = E_{kin}(\kappa,\eta,\omega, z = 0)$.

For annual variations (Fig. 5, top) of the wind field ($\omega = 2 \cdot 10^{-7}$), the response is flat over the entire wave number range with a dominating signal at that wave number ($\kappa \approx 8 \cdot 10^{-7} cm^{-1}$), where the line $\omega = 2 \cdot 10^{-7}$ intersects the dispersion line of the barotropic Rossby wave (ν_o). Thus, if the annual variations of the wind field would contain energy enough at that wave number which corresponds to a wave length of about 78 km, barotropic Rossby waves would be created directly by the wind.

According to Fig. 4 , for periods more than 1 year, baroclinic Rossby waves can be excited in a mid-latitude ocean. For periods of 10 years (Fig. 5, middle) the first mode occurs additionally to the barotropic one, slightly shifted towards higher wave numbers due to friction. The energy of the first mode exceeds the energy level of the surroundings by a factor of approximately 4. Higher modes are not stimulated. When increasing the periods (Fig. 5, bottom) higher modes come into existence.

The response for a fixed κ and a variable ω is displayed in Fig. 6 for $\kappa = 5 \cdot 10^{-9}$, which is the basin scale (L = 6000 km). Due to friction we observe a shift of the resonance peaks towards lower frequencies. Thus, depending on friction, the Rossby waves are expected to occur at locations in the frequency-wave number range obtained by slightly shifting the dispersion lines in Fig. 4 towards the bottom of the figure.

As outlined in I, the ocean responds to each frequency-wave number combination linearly. But the waves are shifted towards west due to the ß-term. Despite the fact that the wind stress $\tau^{(x)}$ fits into the basin, the response does not. To meet the boundary condition we have to add a free solution which amplitude is chosen such as to cancel the forced one with respect to the normal velocity at the coasts.

2.4. The free solution

The system (I.4.4.4) is approximated by central differences. We then have

$$(2.4.1) \quad A \cdot \vec{U}(s+1) + B \cdot \vec{U}(s) + C \cdot \vec{U}(s-1) = 0$$

where

$$(2.4.2) \qquad \vec{U}(s) = (\tilde{\phi}_{n_1}, \tilde{\phi}_{n_2}, \tilde{\psi}_{n_1}, \tilde{\psi}_{n_2}, \tilde{P}_{n_1}, \tilde{P}_{n_2})$$

and

$$(2.4.3) \quad A = \begin{pmatrix} \frac{1}{\Delta x^2} & 0 & 0 & 0 & 0 & 0 \\ 0 & \frac{1}{\Delta x^2} & 0 & 0 & 0 & 0 \\ 0 & 0 & \frac{1}{\Delta x^2} + \frac{\beta k_H}{2\Delta x D} & -\frac{\beta\omega}{2\Delta x D} & 0 & 0 \\ 0 & 0 & \frac{\beta\omega}{2\Delta x D} & \frac{1}{\Delta x^2} + \frac{\beta k_H}{2\Delta x D} & 0 & 0 \\ \frac{\beta}{2\Delta x} & 0 & -\frac{f_o}{\Delta x^2} & 0 & \frac{1}{\Delta x^2} & 0 \\ 0 & \frac{\beta}{2\Delta x} & 0 & -\frac{f_o}{\Delta x^2} & 0 & \frac{1}{\Delta x^2} \end{pmatrix}$$

(2.4.4)
$$B = \begin{pmatrix} -\frac{2}{\Delta x^2} - \eta^2 & 0 & 0 & 0 & 0 & \omega\nu_n \\ 0 & -\frac{2}{\Delta x^2} - \eta^2 & 0 & 0 & -\omega\nu_n & 0 \\ -\frac{\beta\eta\omega}{D} & -\frac{\beta\eta k_H}{D} & -\frac{2}{\Delta x^2} - \eta^2 & 0 & -\frac{\omega^2\nu_n f_o}{D} & -\frac{\omega k_H f\nu_n}{D} \\ \frac{\beta\eta k_H}{D} & -\frac{\beta\eta\omega}{D} & 0 & -\frac{2}{\Delta x^2} - \eta^2 & \frac{\omega k_H f\nu_n}{D} & -\frac{\omega^2\nu_n f_o}{D} \\ 0 & 0 & \frac{2f_o}{\Delta x^2} + f_o\eta^2 & \beta\eta & -\frac{2}{\Delta x^2} - \eta^2 + \omega^2\nu_n & -\omega\nu_n \\ 0 & 0 & -\beta\eta & \frac{2f_o}{\Delta x^2} + f_o\eta^2 & \omega\nu_n & -\frac{2}{\Delta x^2} - \eta^2 + \omega^2 \end{pmatrix}$$

(2.4.5)
$$C = \begin{pmatrix} \frac{1}{\Delta x^2} & 0 & 0 & 0 & 0 & 0 \\ 0 & \frac{1}{\Delta x^2} & 0 & 0 & 0 & 0 \\ 0 & 0 & \frac{1}{\Delta x^2} - \frac{\beta k_H}{D} & \frac{\beta\omega}{2\Delta x D} & 0 & 0 \\ 0 & 0 & -\frac{\beta\omega}{2\Delta x D} & \frac{1}{\Delta x} - \frac{\beta k_H}{2\Delta x D} & 0 & 0 \\ -\frac{\beta}{2\Delta x} & 0 & -\frac{f_o}{\Delta x^2} & 0 & \frac{1}{\Delta x^2} & 0 \\ 0 & -\frac{\beta}{2\Delta x} & 0 & -\frac{f_o}{\Delta x^2} & 0 & \frac{1}{\Delta x^2} \end{pmatrix}$$

The solution of (2.4.1) is obtained by the same procedure as in section 2.2. We define $\alpha(s)$, $\vec{\beta}(s)$, by

$$\vec{U}(s) = \alpha(s) \cdot \vec{U}(s+1) + \vec{\beta}(s) \tag{2.4.6}$$

which - together with(2.4.1) - yields

$$\begin{cases} \alpha(s) = -\left(B(s) + C(s)\cdot\alpha(s-1)\right)^{-1}\cdot A \\ \vec{\beta}(s) = -\left(B(s) + C(s)\cdot\alpha(s-1)\right)^{-1}\cdot C\cdot\vec{\beta}(s-1) \end{cases} \tag{2.4.7}$$

The boundary condition (I.4.5.5) may be written as

$$\vec{U}(1) - \vec{U}(0) + \Delta x\cdot E\cdot\vec{U}(0) = \Delta x\vec{Q}(0) \tag{2.4.8}$$

where

$$E = \begin{pmatrix} 0 & 0 & 0 & \eta & 0 & 0 \\ 0 & 0 & -\eta & 0 & 0 & 0 \\ 0 & -\eta & 0 & 0 & -\frac{\omega\eta}{D} & \frac{\eta k_H}{D} \\ \eta & 0 & 0 & 0 & -\frac{\eta k_H}{D} & -\frac{\omega\eta}{D} \\ 0 & 0 & 0 & 0 & -\frac{\eta\omega f_0}{D} & \frac{\eta f_0 k_H}{D} \\ 0 & 0 & 0 & 0 & -\frac{\eta f_0 k_H}{D} & \frac{\eta\omega f_0}{D} \end{pmatrix} \tag{2.4.9}$$

and

$$(2.4.10)\quad \vec{Q}(0) = \left(-D_{1n}, -D_{2n}, -\frac{f_o k_H}{D} D_{1n} - \frac{f_o \omega}{D} D_{2n}, \frac{f_o \omega}{D} D_{1n} - \frac{f_o k_H}{D} D_{2n},\right.$$

$$\left. -\frac{k_H(f_o^2+D)}{D} D_{1n} - \frac{\omega(f_o^2+D)}{D} D_{2n}, \frac{\omega(f_o^2-D)}{D} D_{1n} - \frac{k_H(f_o^2+D)}{D} D_{2n}\right)$$

From (2.4.6) and (2.4.8) we obtain

$$(2.4.11)\quad \begin{cases} \alpha(0) = (I - \Delta x E)^{-1} \\ \vec{\beta}(0) = -\alpha(0)\,\Delta x\ \vec{Q}(0) \end{cases}$$

which allows to compute $\alpha(s)$ and $\vec{\beta}(s)$ according to (2.4.7) for all s.

At the western boundary $x = X = S\Delta x$, the corresponding vector for (2.4.10) is $\vec{Q}(X)$. From

$$(2.4.12)\quad \vec{U}(S) - \vec{U}(S-1) + \Delta x E \cdot \vec{U}(S) = \Delta x \vec{Q}(X)$$

and (2.4.6) we obtain

$$(2.4.13) \qquad \vec{U}(S) = (I - \alpha(S-1) + \Delta x E)^{-1} \, (\Delta x \vec{Q}(X) + \vec{\beta}(S-1))$$

which allows to calculate the remaining $\vec{U}(s)$ in decreasing order by means of (2.4.6). Thus, the free solution is completed.

2.5. Eigenfunction expansion

The eigenfunctions (I.4.1.3) of the system

$$(2.5.1) \qquad \frac{d}{dz}\left[\frac{1}{g\Gamma}\left(\frac{dZ_n}{dz} + \Gamma Z_n\right)\right] + \nu_n Z_n = 0$$

subject to

$$(2.5.2) \qquad \frac{dZ_n}{dz} = 0 \quad \text{at } z = 0 \quad \text{and } z = H$$

are computed by standard methods with $\Delta z = 20$ m. They are displayed in Fig. 7 for the lowest orders.

3. Examples

As outlined in I, time stepping methods require a large amount of computer time by integrating the hydrodynamic equations even in the linear case. The advantage of the present model is most pronounced in the range of Rossby

waves where a few frequencies and wave numbers of the forcing function are sufficient to simulate the response of the ocean. A few examples may serve to demonstrate this.

Applications to real wind fields will be given elsewhere (KRAUSS & WÜBBER, 1982).

We use a midocean basin X = 6280 km east-west and Y = 3140 north-south extension. The depth is 4000 m. Stratification and eddy viscosity are displayed in Fig. 3. Some selected eigenfunctions are shown in Fig. 7. Bottom friction is chosen to be r = 0,1. The forced solution is obtained by solving the equations with Δz = 20 m. 21 eigenfunctions (ν_o - ν_{20}) have been used to approximate the forced solution at the boundaries, but 11 eigenfunctions turn out to be sufficient in most cases. The zero crossings of mode number 20 are in 13, 37, 60, 84, 108, 137, 170, 220 m. Thus, the vertical resolution of the model may be considered to be 25 - 50 m, increasing with depth. With respect to the horizontal direction x, the resolution is given by the free solution. The forced one reveals all features due to the wind field. For the free one we generally use 200 grid-points in x-direction which gives a resolution of 30 km. From the results we take the mean values for 10 layers. In the present case they have a thickness of 400 m, thus extending from 0 - 400 m, ..., 3600 - 4000 m. The results are displayed for t = 0.

3.1. The response to annual forcing

As a test field we use

(3.1.1) $\tau^{(x)} = \cos \eta y \cos \omega t \qquad \tau^{(y)} = 0$

The constancy with respect to x is approximated by a Lanczos-filtered sine expansion (see Fig. 2) with 11 wave numbers. The computing time amounts to about 60 sec on a CYBER 76.

Fig. 8 displays the average over the entire water column, the currents are shown at the top, the lower panel displays the pressure field. Maximum current speeds are 22.1 cm sec^{-1} at the western coast which corresponds to a mass transport of 62.4 Sv within the western boundary current. Within the Ekman layer the current speed is slightly increased and the currents are deflected somewhat to the right. The figure is not shown here. In all deeper layers the currents are the same as in Fig. 8. Thus, the ocean responds barotropically, as expected from the dispersion lines (Fig. 4).

If we increase the period, we still remain in the gap between barotropic and baroclinic Rossby waves and, consequently, the response remains the same. For periods of 2 years, the maximum currents are 22.9 cm sec^{-1}, for 4 years 23.3 cm/sec. It may be mentioned that the location of this gap strongly depends on the geographic latitude where the ß-plane is attached. In the present case this happens at $\phi = 45^{\circ}N$. Thus, our ocean extends from about $30^{\circ}N$ through $60^{\circ}N$, and the forcing is due to low wave numbers only. For a description of the real conditions the ß-plane should be attached at

about 30°N and high wave numbers must be included. In this case the ocean may show a baroclinic response even at a forcing period of 1 year (KRAUSS & WÜBBER, 1982).

3.2. Forcing in the range of baroclinic Rossby waves

The solutions become different if we choose periods within the range of baroclinic Rossby waves. Fig. 9 displays the vertically averaged solution (upper panels) and the solution in the upper 400 m (lower panels) at a period of 20 years.

Large-scale Rossby waves are superposed on the gyre in this case. They are dominated by the first mode, as shown by Fig. 10 for the maximum speed within the western boundary current. The mass transport of this boundary current is 70.7 Sv, its width is 390 km.

Similar results (but different patterns) are obtained for the entire period range from a few years up to several 100 years. The results are not sensitive to bottom friction and chosen eddy viscosity.

3.3. Quasi-steady forcing

If the period is further increased, one finally would expect a quasi-steady response. This, however, shows very peculiar features and seems to have been overlooked in the past.

For continuous stratification the inviscid problem was first discussed by CHARNEY & FLIERL (1981) and has been further elucidated by YOUNG (1981). The entire current is concentrated at the top of the inviscid interior layer.

The structure of the currents in the viscous surface layer was mentioned already in connection with (I.3.1.12). The stream function of the forced solution is approximately given by

$$(3.3.1) \qquad \psi \sim e^{-(1+i)\sqrt{\frac{\beta\kappa}{2\mu k^2}}\, z}$$

For reasonable eddy viscosities ($\mu \approx 100$) the circulation in ocean wide gyres would be limited to the upper 100 m. This has been recognized in linear, layered models already where the momentum of the wind field is transferred to the top layer only if eddy viscosity is small in the interior. The pressure field of the sea surface is cancelled by a deflection of the internal boundary.

The solution then depends entirely on $\mu(z)$. As an example we choose a forcing period of 10^5 years. The results are shown in Fig. 11 displaying the currents averaged over the entire water column (top panels) and for the layer 0 - 400 m. The current is less than o.1 cm/sec^{-1} below 400 m. The western boundary current is entirely concentrated on the surface layers . Averaged over the upper 400 m, it reaches 995 cm/sec, but the mass transport in the entire water column (top panels) amounts to 44.6 Sv only. Thus, the model is still appropriate to calculate the vertically averaged transport but fails to give a reasonable vertical distribution.

The reason for it must be seen in the incompressitility condition

$$\frac{\partial R}{\partial t} + \Gamma w = 0 \qquad (3.3.2)$$

which fails to describe the density advection correctly at very low frequencies. For very long periods vertical mixing must be included. Horizontal advection does not seem to change the solution markedly (YOUNG,1981). The problem will be dealt with in a separate paper.

4. Conclusions

The model is able to calculate the response of a stratified ocean to external forcing in the entire frequency domain of the barotropic and baroclinic Rossby waves. For steady forcing - which can be described by superposition of several frequencies (Fourier expansion into odd harmonics of a wind constant over a time range $0 \leq t \leq T$ and changing sign for $T \leq t \leq 2T$) no steady state is obtained. This is due to (3.3.2).

Constant wind produces constant Ekman pumping ($w>0$) and, thus, yields a linear change in density which in turn changes the pressure field (static equation). In order to obtain steady solutions we must include vertical mixing of density.

The model allows very high vertical and horizontal resolution and requires much less computer time than any time stepping model with such resolution would require.

References

GODIN, G., 1972: The analysis of tides. Liverpool University Press, 264 pp.

HOLLAND, W.R. and L.B. LIN, 1975: On the generation of mesoscale eddies and their contribution to the oceanic general circulation. J. Phys. Oceanogr. 5, 642 - 669.

KRAUSS, W., 1976: On currents, internal and inertial waves in a stratified ocean due to variable winds. Part 1. Dtsche Hydrogr. Z. 29, 87 - 96.

KRAUSS, W. and Chr. WÜBBER, 1982: The response of the North Atlantic tc annual wind variations along the eastern coast. Deep-Sea Res., 29, 851-868.

LINDZEN, R.S. and H.-L. KUO, 1969: A reliable method for the numerical integration of a large class of ordinary and partial differential equations. Month. Weather Rev. 97, 732.

RICHTMYER R.D. and K.W. MORTON, 1967: Difference methods for initial-value problems. Sec. Ed. Interscience Publ. New York, 405 p.

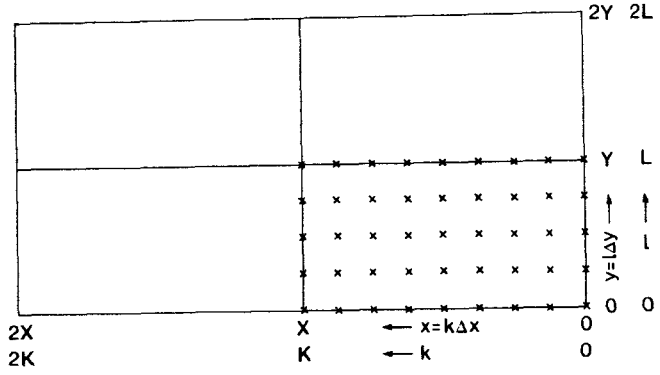

Fig. 1 Part 2 Real ocean basin $0 < x < X$, $0 < y < Y$ and Fourier expansion domain $0 < x < 2X$, $0 < y < 2Y$.

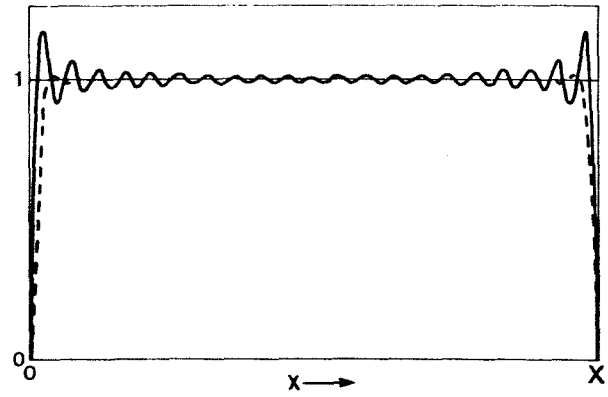

Fig. 2 Part 2 Approximation of 1 in $0 < x < X$ by 20 Fourier sine waves before (full line) and after Lanczos filtering (dashed line).

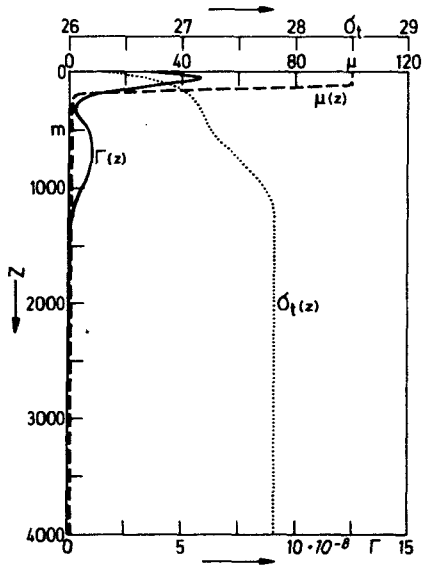

Fig. 3 Density σ_t, stability Γ and eddy viscosity μ as functions
Part 2 of depth. (Γ and μ in cgs-units)

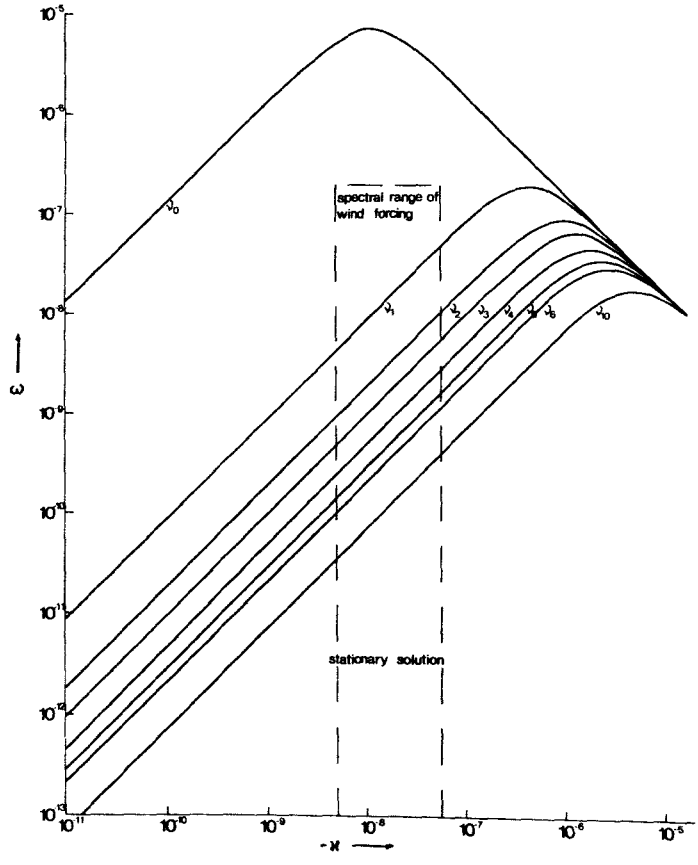

Fig. 4 Part 2 Dispersion curves for barotropic (ν_0) and baroclinic (ν_1 - ν_{10}) Rossby waves

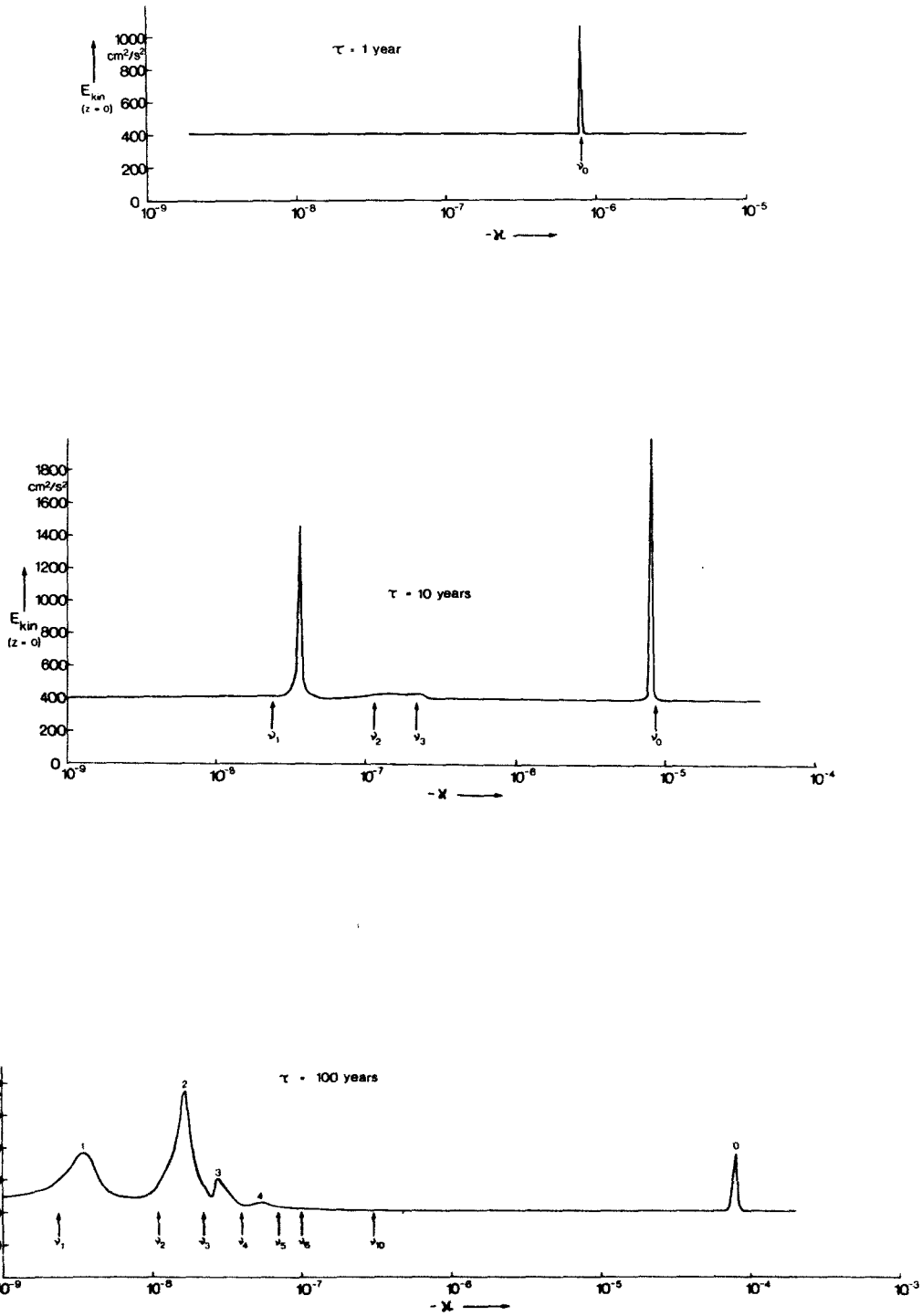

Fig. 5 Part 2 Response function $E_{kin}(z = 0)$ due to a windstress $\tau^{(x)} = 1$ and a forcing period of 1 year (top), 10 years (middle) and 100 years (bottom) as function of wave number κ.

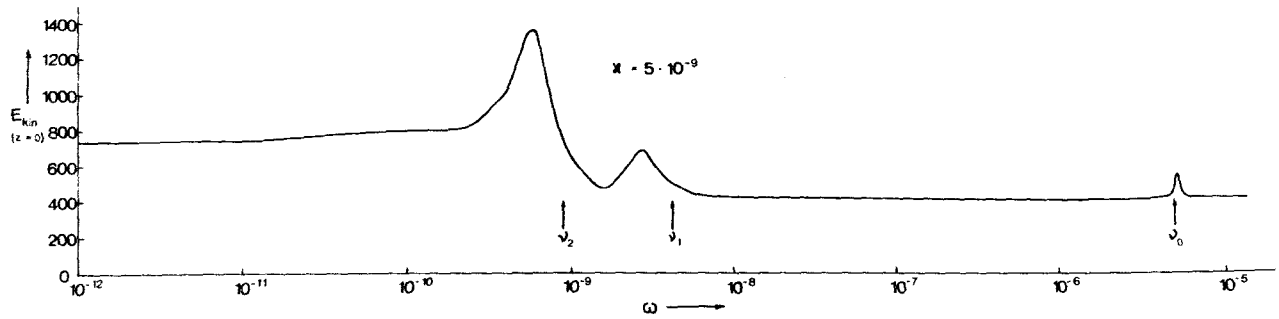

Fig. 6 The same as fig. 5, but as function of ω for fixed
Part 2 $\kappa = 5 \cdot 10^{-9}$ (basic Fourier component)

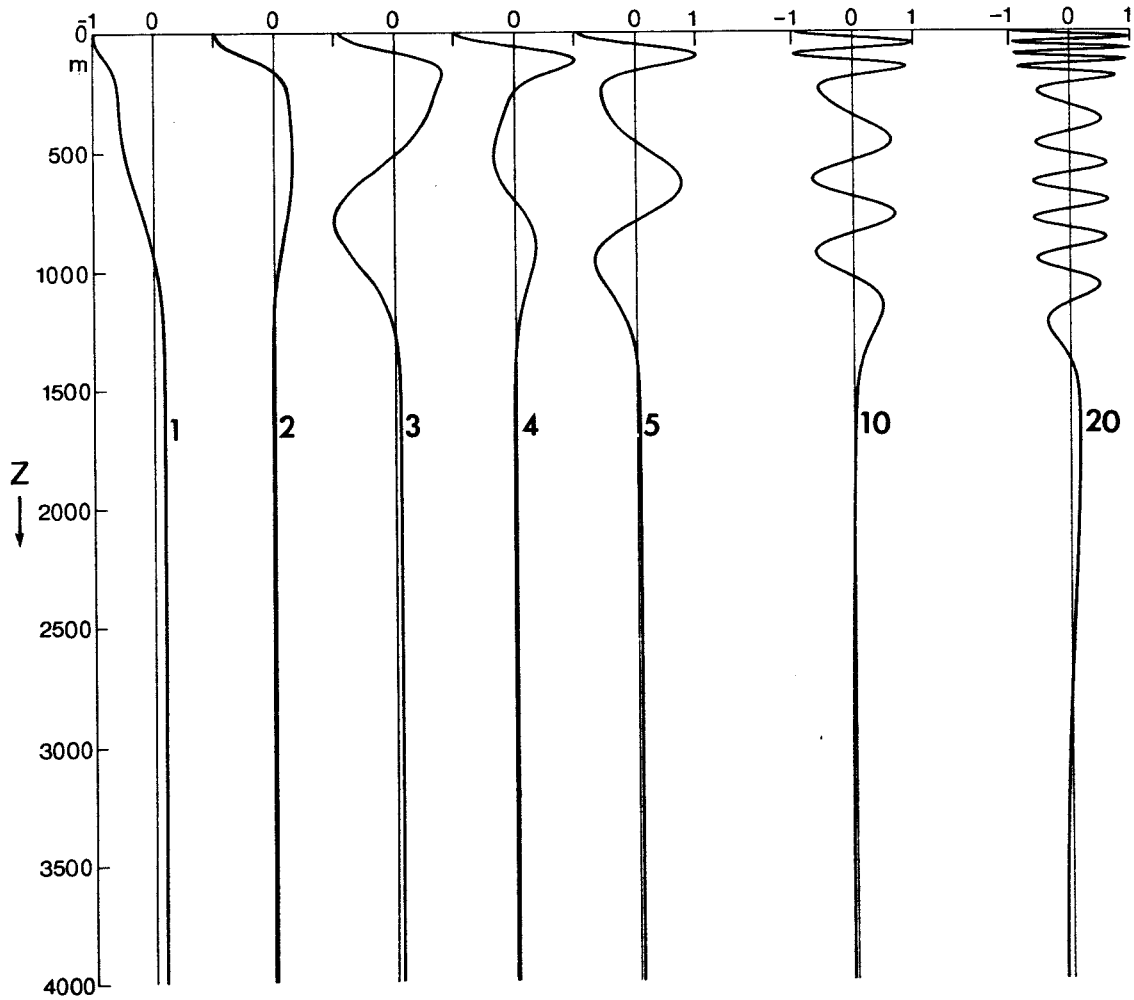

Fig. 7 Part 2 Eigenfunctions due to the stratification of fig. 3. The numbers refer to the order.

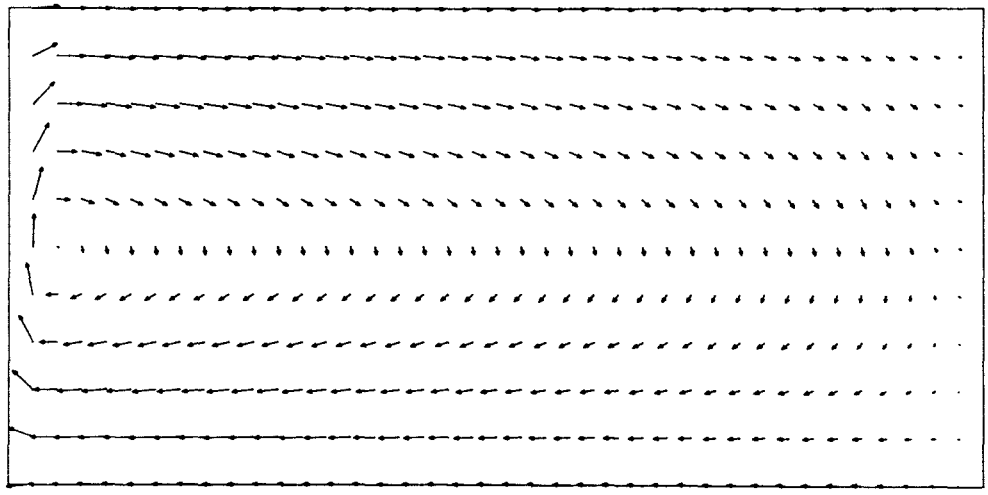

⟶ := 2cm/s

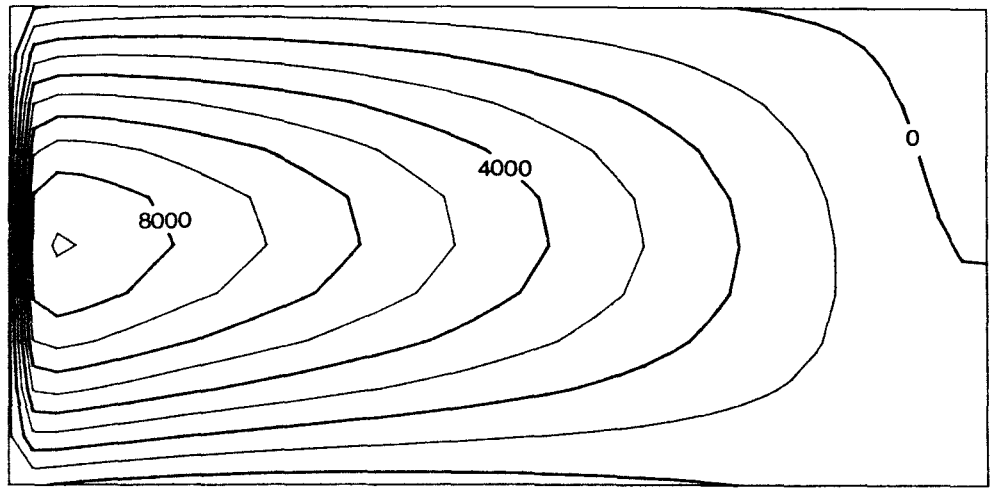

Fig. 8 Part 2 Vertically averaged current (top) and pressure field (bottom) for a forcing period of 1 year. (The arrows along the western boundary have been omitted. Pressure units are $cm^2 s^{-2}$. The vertical displacement in cm is obtained by multiplication with $g^{-1} \approx 10^{-3}$ at z = 0.)

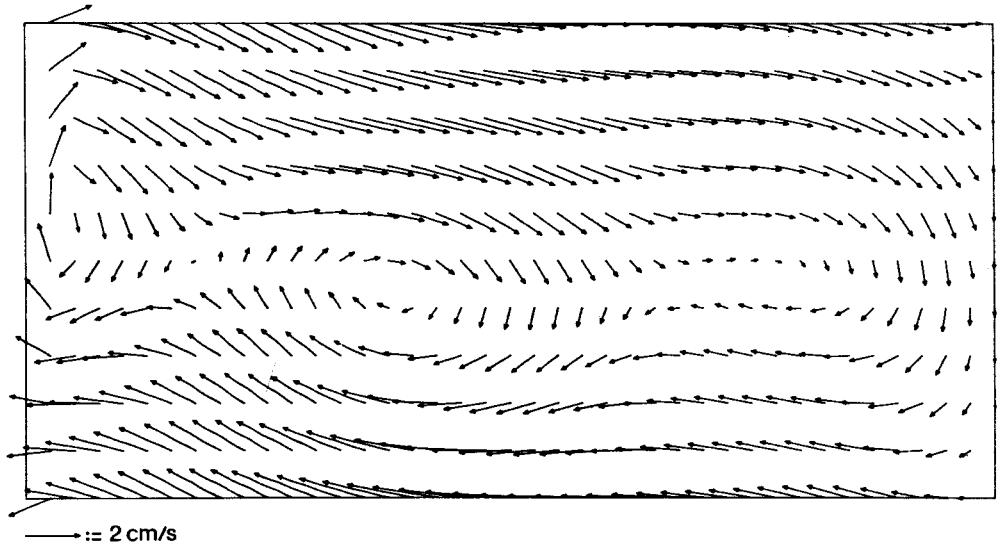

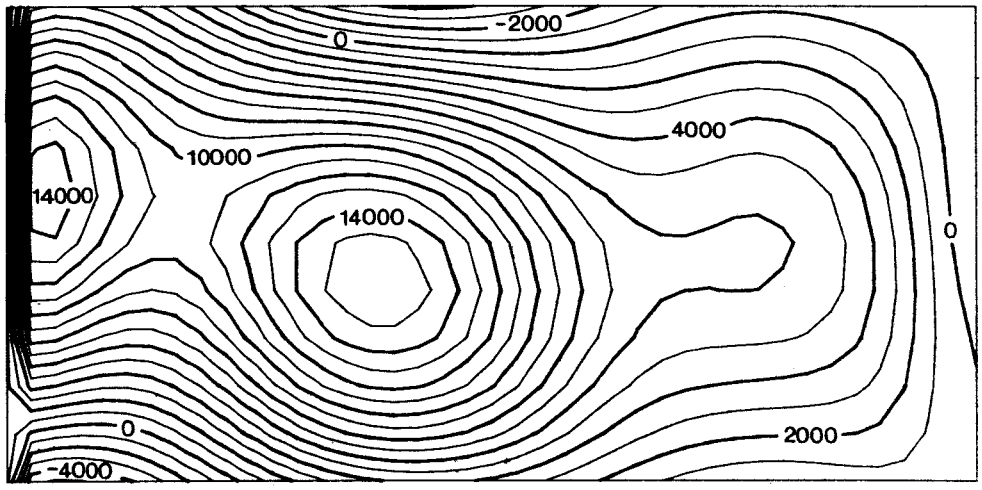

Fig. 9 Part 2 — Vertically averaged currents (0 - 4000 m) and associated pressure field (top panels) and currents and pressure in the layer 0 - 400 m for a forcing period of 20 years. (The arrows along the western boundary have been omitted. Pressure units as in Fig. 8) - lower panel -

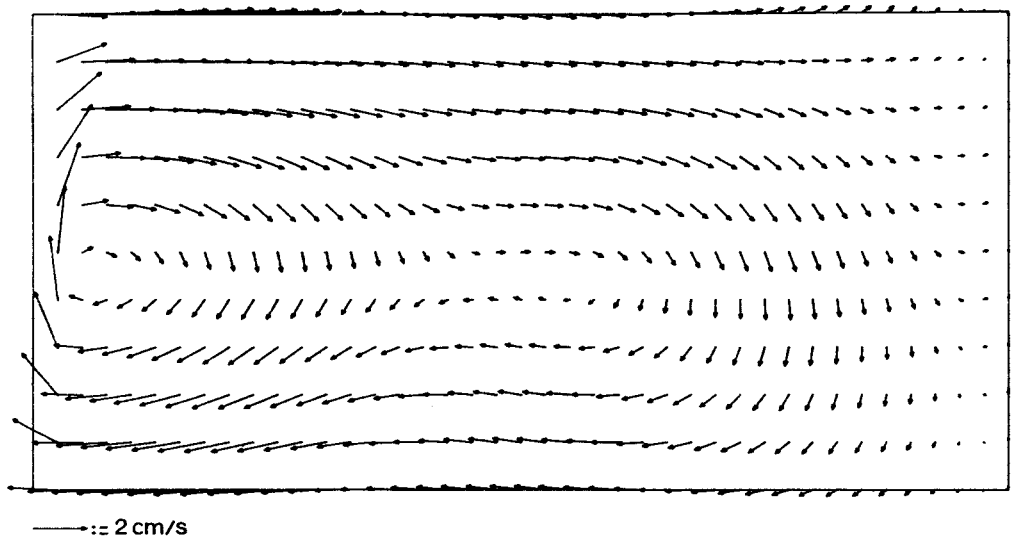

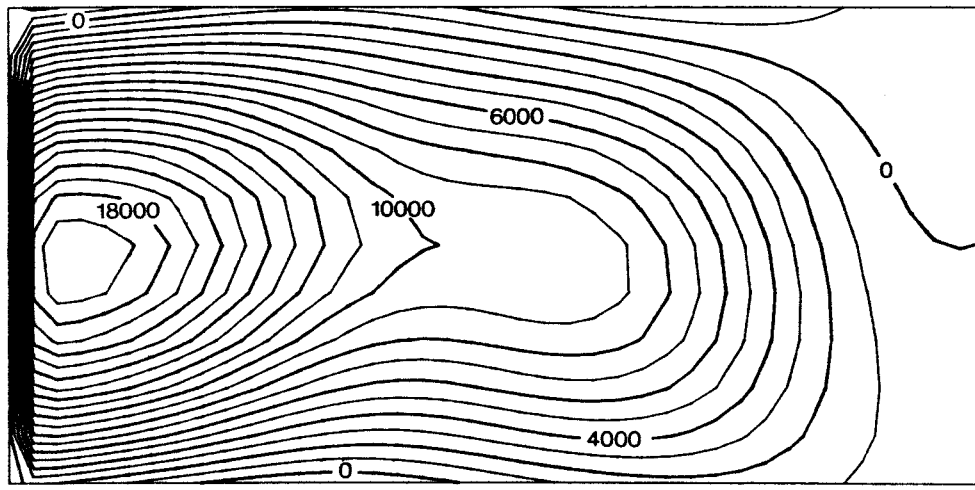

Fig. 9 Part 2 Vertically averaged currents (0 - 4000 m) and associated pressure field (top panels) and currents and pressure in the layer 0 - 400 m for a forcing period of 20 years. (The arrows along the western boundary have been omitted. Pressure units as in Fig. 8.) - upper panel -

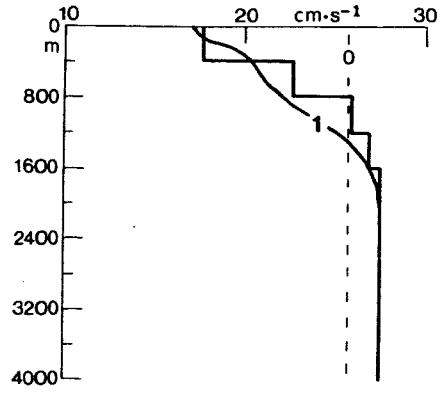

Fig. 10 Part 2 Velocity component v(z) for the 10 layers in the western boundary current (step line); Mode number 0 (dashed line) and 1 (full line). . Forcing period 20 years.

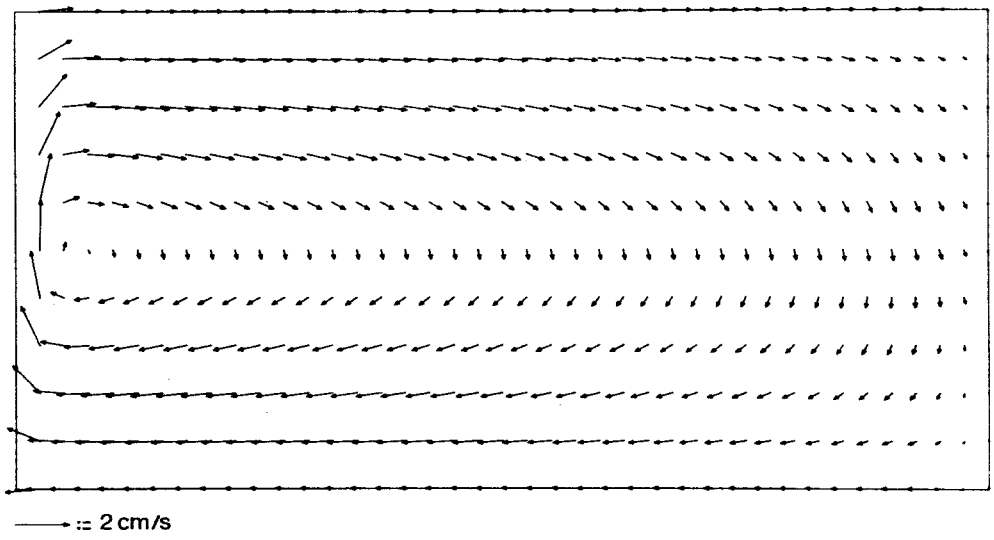

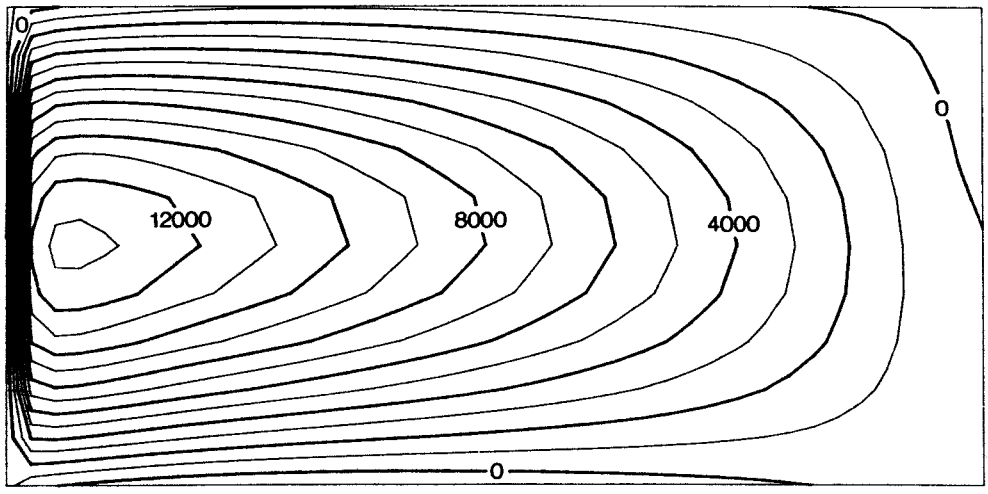

Fig. 11 Part 2 The same as fig. 9 for a forcing function of 10^5 years.
- upper panel -

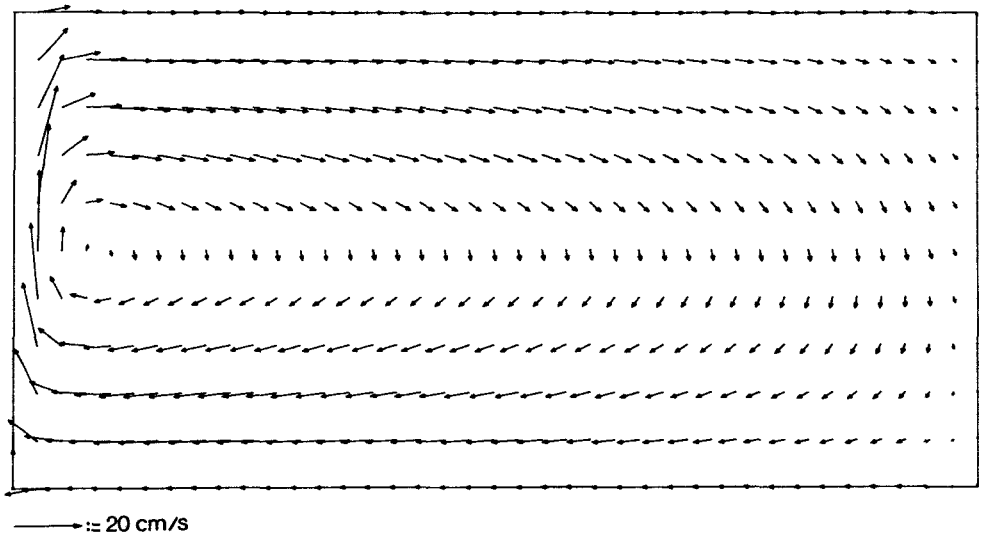

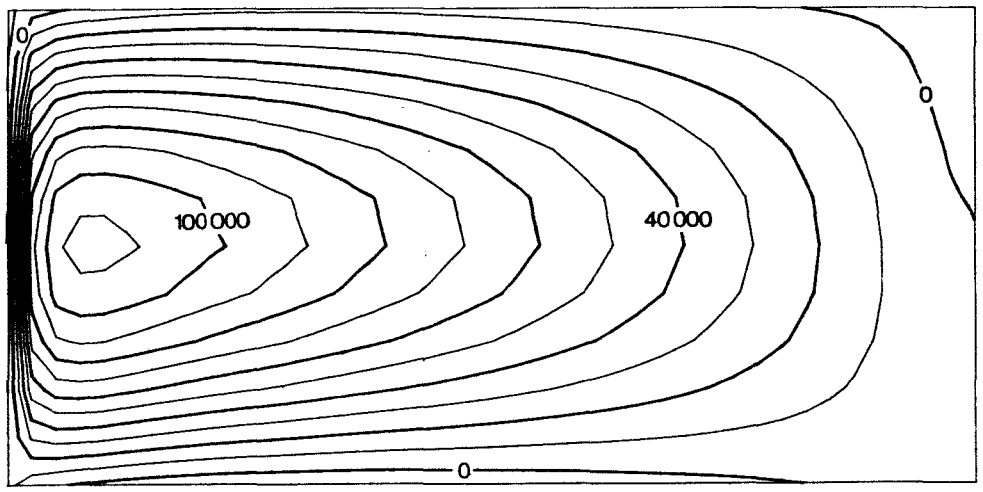

Fig. 11 The same as fig. 9 for a forcing function of 10^5 years.
Part 2 - lower panel -